Anode Material Testing in a Vacuum Diode

by

John Vara, B.S.E.E

A Thesis

In

ELECTRICAL ENGINEERING

Submitted to the Graduate Faculty
of Texas Tech University in
Partial Fulfillment of
the Requirements for
the Degree of

MASTER OF SCIENCES

IN

ELECTRICAL ENGINEERING

Approved

Dr. James Dickens
Committee Chair

Dr. John Krile

Peggy Miller
Dean of the Graduate School

May, 2011

ACKNOWLEDGMENTS

First, I would like to thank my committee members. Thank you, Dr. Dickens, for giving me the opportunity to work in such a great lab at Texas Tech University. Dr. Krile, thank you for your guidance and suggestions throughout my thesis work. Special thanks to John Walter for guiding me through this project and all the help teaching me how to build the vircator countless times. Also, thanks to the undergrads, Chris and Ben, for help bolting the vircator together. Thank you to my family for all their love and support throughout my academic career. I would not be here without you, so thank you. Thank you to my parents for instilling in me the will to succeed and giving me encouraging words when I needed them. Finally, thank you to Danny Garcia, Dino Castro, and Joel Perez for helping me throughout this project. Thank you, Lee Waldrep, for machining parts for me. Thanks to my colleagues in the Lab for making The Center for Pulsed Power and Power Electronics such a great place to be working.

TABLE OF CONTENTS

ABSTRACT

The gases evolved during the operation of a virtual cathode oscillator (vircator) can be detrimental to its maximum output power, repetition rate, and pulse width. Gases are known to evolve both from processes at the cathode, such as explosive electron emission, and anode processes such as heating by the electron beam. A residual gas analyzer (RGA) and pressure measurements have been used to perform characterization of background gases before and after the operation of the vircator. Multiple anode materials have been tested, with measurements made of both the quantity and types of gases evolved during firing. The test materials include stainless steel, copper tungsten, tantalum, nickel, molybdenum and oxygen-free high-conductivity copper. For nickel, two anodes are machined and given different treatments before operation in the sealed vircator. The first being a high temperature bake-out under vacuum (10^{-7} Torr) followed by an ultrasonic cleaning. The second treatment omits the high temperature bake-out. A low impedance Marx generator, with no intermediate pulse forming apparatus, is used to drive the vircator. For all testing, an aluminum cathode is used. The pressure measurement systems and diagnostics are described, and gas analysis and composition are presented for multiple anode materials.

LIST OF TABLES

LIST OF FIGURES

CHAPTER I

INTRODUCTION

High power microwave devices have been the topic of much research. One such device is called the virtual cathode oscillator (vircator). Vircators require no external magnetic field making them generally robust and simple to build [1]. Frequencies, for the vircator, range from 1 to 10 gigahertz (GHz) with output power in the gigawatt regime. Vircators are space-charge driven devices utilizing the formation of a virtual cathode [1]. Gas evolution inside the vircator decreases output power, pulse width, and maximum repetition rate. The goal of this project is to test and analyze different anode materials used in a reflex triode vircator. A residual gas analyzer (RGA) probe is placed inside the vircator stainless steel vacuum tube and is used to measure and characterize any gases inside. The RGA also monitors pressure changes with the built in ion gauge. A 20 l/s ion pump is used to pump the vacuum tube down to the ultra high vacuum (UHV) for a baseline pressure of ~10^{-8} Torr. Driving the vircator is an eight stage low-impedance Marx generator. A capacitive voltage probe and Pearson coil are used to monitor voltage and current respectively. Figure 1.1 shows a diagram of the set-up with the vircator, Marx generator, and RGA.

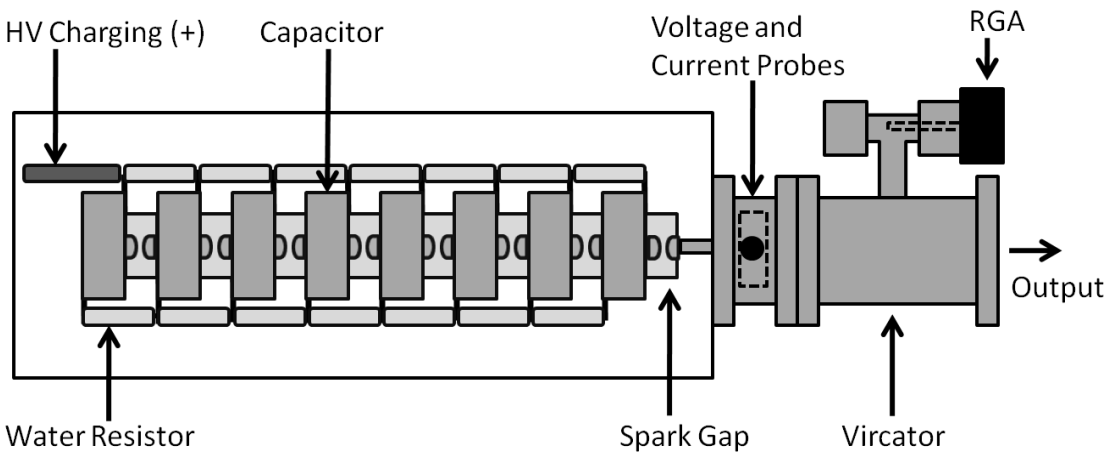

Figure 1.1: Vircator with Marx generator and RGA

Background

Previously, V. D. Selemir et al. studied the microwave generation in a vircator based on the vacuum conditions. V. D. Selemir et al. found that ionization of the residual gas present at higher pressures by the electron beam leads to virtual cathode degradation and decreased efficiency [2]. During operation of the vircator, an electron beam impacts the surface of the anode material causing gases trapped on the surface or in bulk of the anode to be released. The release of gases results in a loss of vacuum quality and therefore loss in performance of the vircator. Residual gases are minimized by high temperature bake out under vacuum, but still remain a problem. Previous research efforts at Texas Tech University have been directed towards vircator cathode optimization by testing cathode materials such as velvet, carbon fiber, solid metal, and pin arrays [5]. For this research, the cathode used is solid aluminum with machined grooves similar to the cathode described in [6], except a Bruce profile is substituted for a previously radial edge. Similar outgassing measurements have been done with a RGA and are described in [2]

and [3]. In both cases, a RGA is used to measure the residual gases present before and after operation of a high power microwave device. Similar efforts were made to approximate molecules generated by assuming the ideal gas law. From Umstattd, Schlise, and Wang, identical cesium iodide coated carbon fiber cathodes were tested with a 90% transparent molybdenum wire mesh anode and carbon microfiber anode insert [2]. Litz, Judy, and Lazard use various cathode materials for gas evolution testing including carbon fiber, velvet, copper, and stainless steel [3]. For this project, the anode materials tested include stainless steel (SS), copper tungsten (CW55), tantalum (Ta), nickel (Ni), molybdenum (Mo), and oxygen-free high-conductivity copper (OFHC copper), which are listed in Table 1.1 along with some properties.

Table 1.1: List of materials [11]

Material	Content	Density (g/cc)	Resistivity (μΩ*cm)	Thermal conductivity (W/m*K)	Melting Point (˚C)
Stainless Steel 304	70Fe:18:Cr:8Ni	8	72	16.2	1454
Copper Tungsten CuW55	55W:45Cu	12.5	0.319	150	3240
Tantalum	99.95Ta	16.7	13.5	54.4	3017
Nickel 201	99Ni	8.89	0.096	70.3	1435
Molybdenum	99.95Mo	10.2	5.34	146.5	2617
OFH Copper	99.99Cu	8.91	0.017	387	1084

CHAPTER II

RESIDUAL GAS ANALYZER

A residual gas analyzer (RGA) is utilized to measure the gases evolved from the electrode materials inside the vircator. The RGA is a quadrupole mass analyzer with built in pirani and ion gauge from Extorr model XT100M. It is capable of measuring 1 to 100 atomic mass units (amu), where amu refers to 1/12 the mass of a single atom of Carbon-12 [7]. The RGA also has an added electron multiplier, increasing its partial pressure sensitivity down from 10^{-11} to 10^{-14} Torr. The XT100M was preferred over other RGAs because of its unique features listed below. The built in pirani and ion gauge protect the dual thoria coated filaments from loss of vacuum during operation. This is of importance, given that firing the vircator may cause the system to over pressure suddenly. The RGA also has 3 modes of operation; analog, trend, and leak detect. The analog mass scans are exported as a table of data points to be analyzed later in this paper. Trend mode allows for up to 10 mass numbers to be monitored over time. The data for trend mode is also exported as a table of data points. Leak detect mode allows for helium leak detecting of the vircator. This eliminates the need for a separate helium leak detector and allows for quick detection of any leaks present in the system. Figure 2.1 shows the pressure change in the vircator while being pumped down by the ion-pump after firing a shot with a tantalum anode.

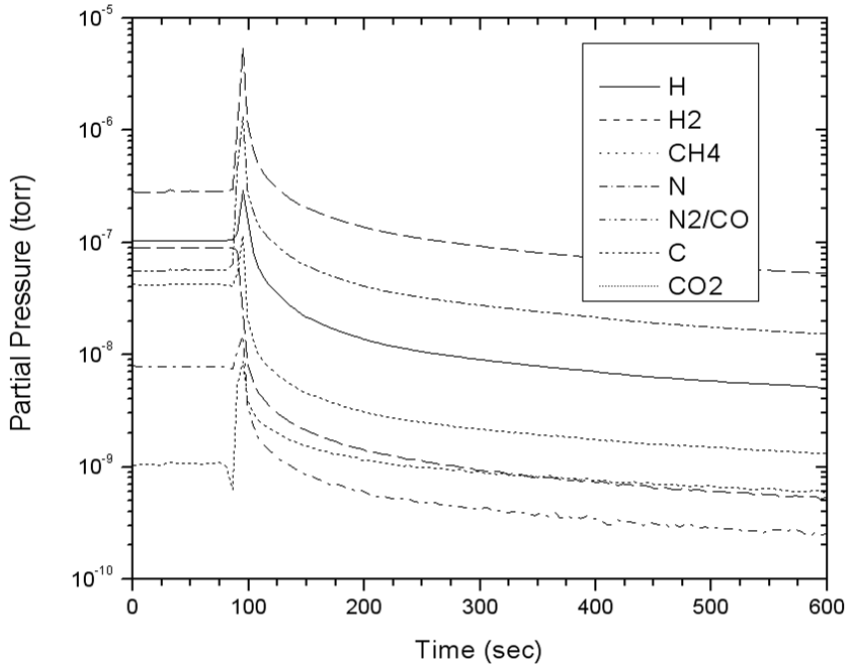

Figure 2.1: Ion-pump down curve after vircator operation with a tantalum anode.

The time at zero seconds corresponds to an initial delay from the RGA boot loading and taking a post shot mass scan. A complete mass scan takes approximately eight seconds to complete and immediately after the RGA is set to trend mode. The trend data represents the partial pressures of the specific amu selected when the ion pump is turned on after approximately 100 seconds corresponding to the spike seen in Figure 2.1.

RGA Operation

The RGA operates by ionizing any residual gases in the vacuum system and directs them through a mass filter to a collector. At the collector, the partial pressures of the ionized gases are measured based on the charged ions. Figure 2.2 shows the ionizer assembly of the RGA from Extorr.

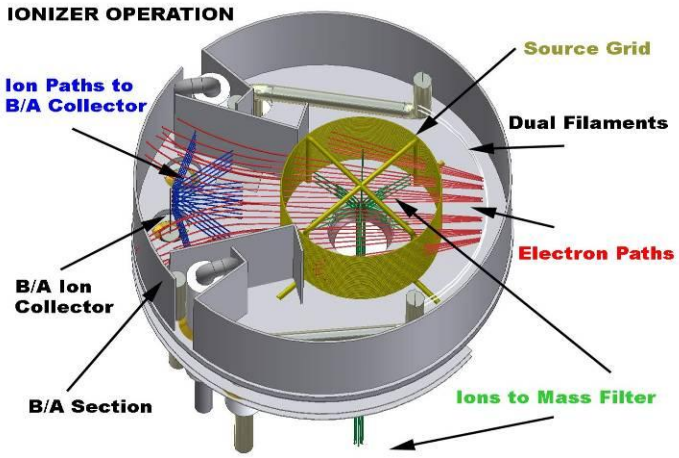

Figure2.2: Ionizer assembly from Extorr [10]

Dual thoria coated iridium filaments at 70eV and 2.0 mA provide the source for electron impact ionization. The ions are then directed towards the quadrupole mass filter, where varying voltages are applied at precise amplitudes and frequencies. After passing through the mass filter, the ions are focused towards a Faraday cup detector where the partial pressure of a particular mass is proportional to the measured ion current [10]. Figure 2.3 shows a schematic drawing of the ion path from ionizer to collector.

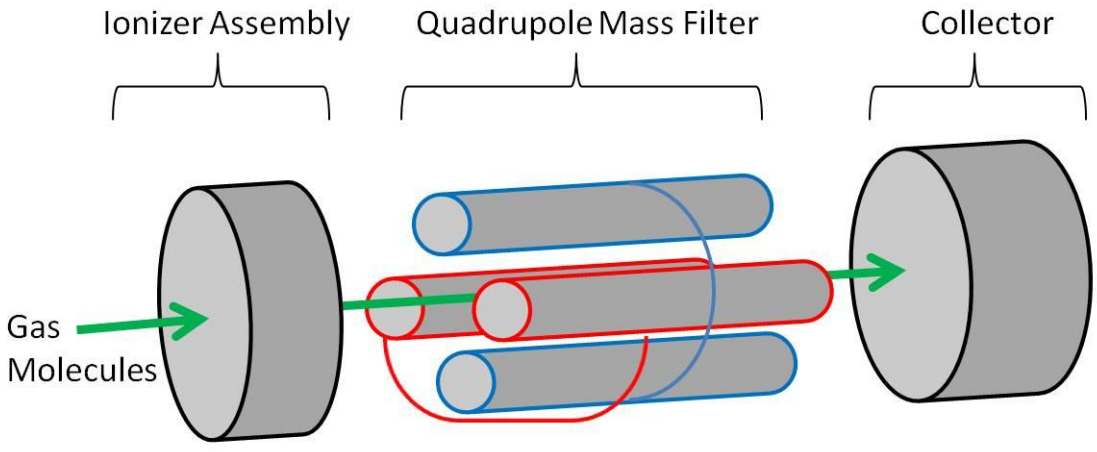

Figure 2.3: Schematic drawing of RGA probe

CHAPTER III

TEST SETUP

The high vacuum portion of the test setup consists of the RGA probe, ion pump, vircator housing, anode, cathode, and high voltage ceramic feed through. This section is brought to high temperatures while under vacuum for at least 24 hours after each tear down and reassembly. This section is then attached to another section containing a capacitive voltage probe and B-dot probe. The assembly is then mounted to the oil containment vessel and connected to the 8 stage Marx generator. A Pearson coil is placed along the ground return strip of the Marx bank.

Marx Generator

A Marx generator is a bank of capacitors connected together in parallel through a resistive network and in series by a series of switches, typically spark gaps. The present Marx utilizes pressure triggered spark gaps. Figure 3.1 shows a top view of Marx generator in transformer oil containment vessel.

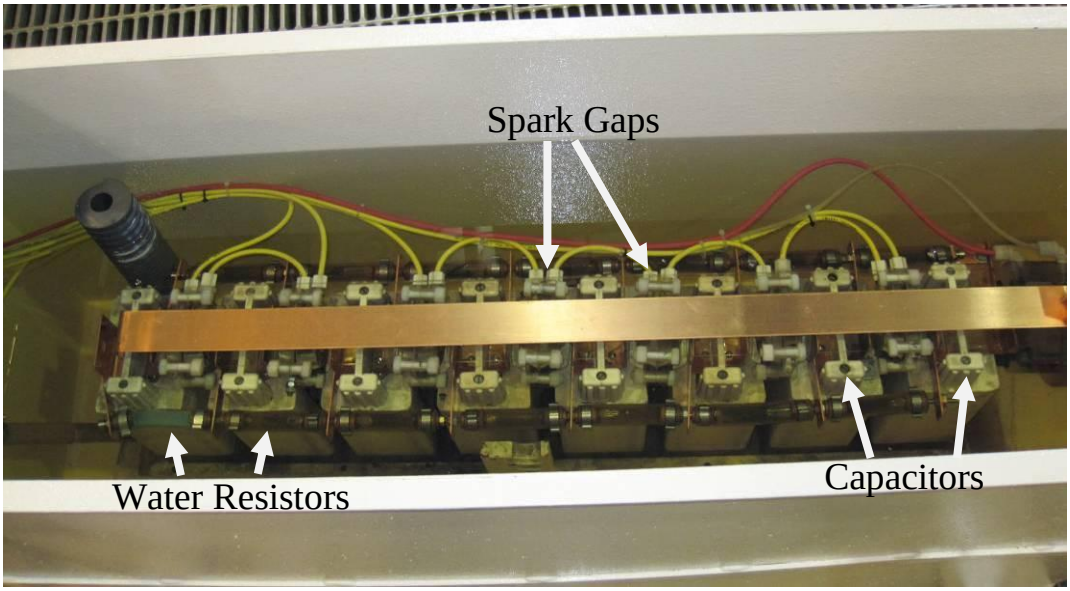

Figure 3.1: Top view of Marx generator used for testing

The Marx generator used for testing is described previously in a thesis paper by Mathew Lara with some modifications to the resistors and copper connectors [8]. The generator consists of eight *Maxwell 31885* 0.1 µF capacitors rated for 75kV. The capacitors are charged to 40kV for each shot, which allows for an ideal maximum output of 320kV to the anode of the vircator. Figure 3.2 shows typical voltage and current waveforms from the Marx generator into the vircator.

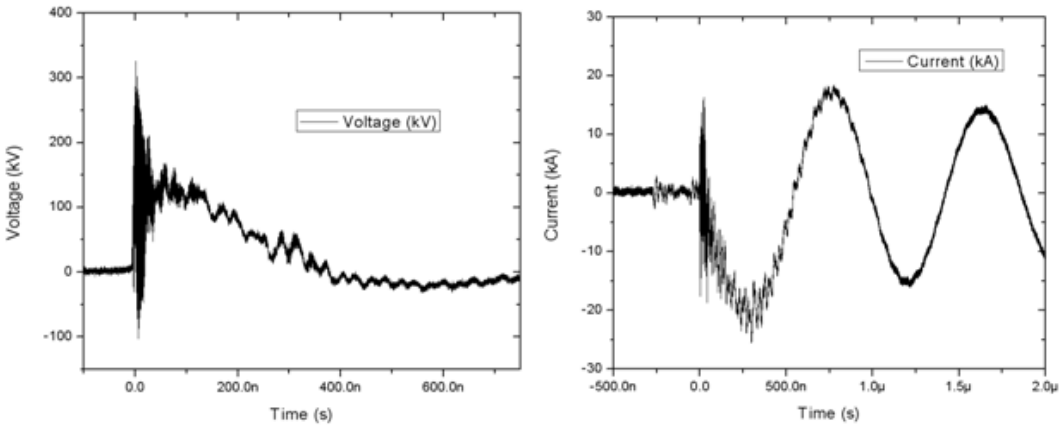

Figure 3.2: Typical voltage and current waveforms

Test Procedures

Before taking an initial RGA scan, the ion pump is turned off and the vircators pressure is allowed to settle and reach equilibrium. The initial scan allows for a baseline pressure reading and reveals any residual gases inside the sealed vircator after bake out. After the vacuum has settled in the UHV range (~10^{-8} Torr), the total pressure and mass sweeps are taken with the RGA. The built-in electron multiplier (EM) allows for increased sensitivity, so one mass scan is taken with the EM off and another with the EM on. Before firing, the RGA's communications and control unit (CCU) is removed to prevent damage to the sensitive electronics. After firing, the CCU is placed back on the system and a complete scan is taken with the ion pump left off. There is approximately 15 seconds delay in the initial start up of the RGA until the first scan is taken. The delay includes the time it takes to place the CCU back on the system and time for the RGA to boot load. This will lead to small errors in the pressure change measurements, but they are only used to make approximate calculations for the number of molecules evolved during the operation of the vircator. The mass sweep for each anode material is saved as a set of data points to be graphed in ORIGIN 8® software. Figure 3.3 shows a picture of an initial mass scan with a nickel anode on a linear scale.

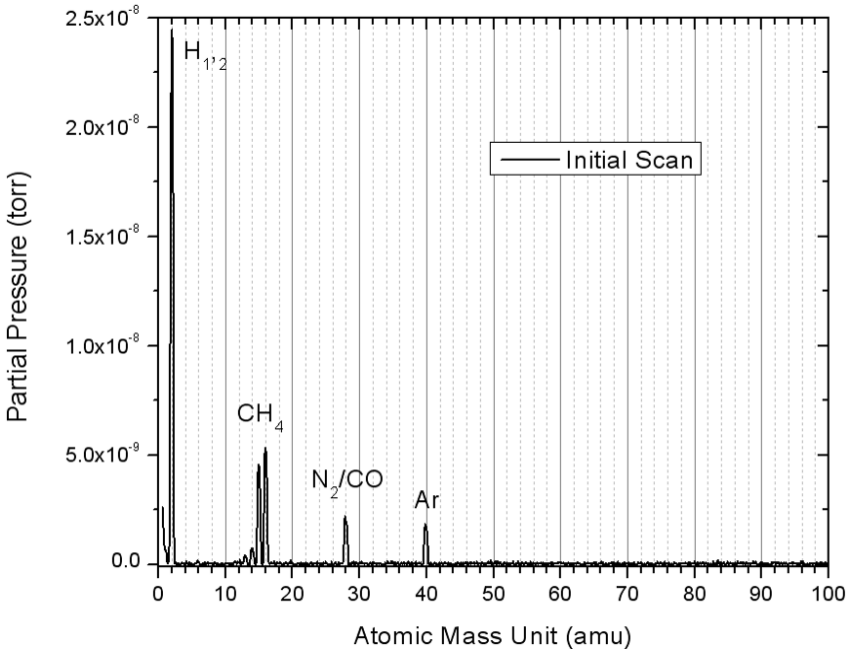

Figure3.3: Initial RGA scan with nickel anode

The initial scan reveals traces of Hydrogen (H_2), methane (CH_4), nitrogen (N_2), carbon monoxide (CO), and argon (Ar) inside the vacuum system. The peak for hydrogen accounts for the highest partial pressure inside the vacuum system, which is typical of stainless steel chambers.

Reflex Triode Vircator

The reflex triode geometry is utilized for testing the different anode materials inside the vircator. In the reflex triode geometry, the anode is pulsed with high voltage and the cathode is grounded. The electron beam generated by the cathode passes through the anode mesh to the virtual cathode where it is reflected back [1]. Figure 3.4 shows the typical configuration for the reflex triode vircator used in testing.

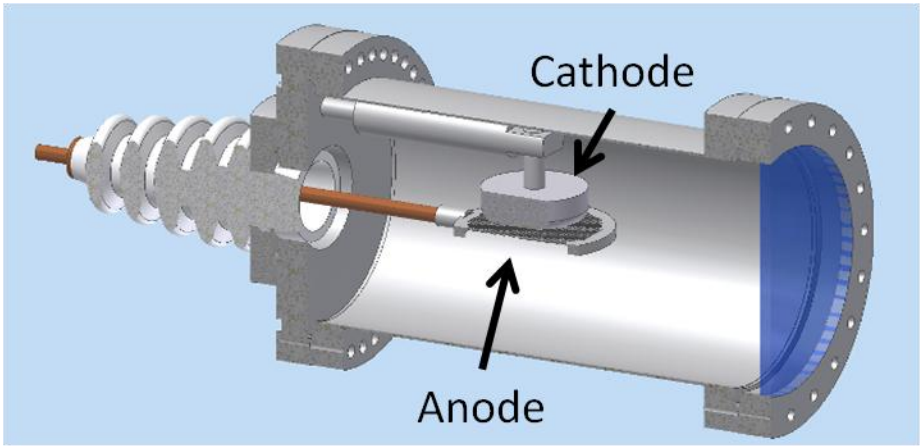

Figure 3.4: Schematic drawing of reflex triode vircator [6]

The vircator chamber is an 8 inch diameter stainless steel tube sealed with Conflat copper-gasket flanges. A distance of 8mm is set for the anode-cathode (A-K) gap during assembly and for all experiments. Each anode is machined from a 4 inch by 12 inch by 0.5 inch plate of the materials listed previously. Figure 3.5 shows a complete anode and cathode before being placed in a vircator.

Figure 3.5: Machined aluminum cathode and copper tungsten anode

The anode has an outer diameter of 3.75 inches and an inner diameter of 3.25 inches and is machined down to a thickness of approximately 25 mils. Hundreds of 0.125 inch holes are drilled through the anode to create a mesh of approximately 70% transparency. The cathode is aluminum and has been described previously. Figure 3.6

shows the vircator attached to the Marx generator with the ion pump and RGA mounted to the right of the output window.

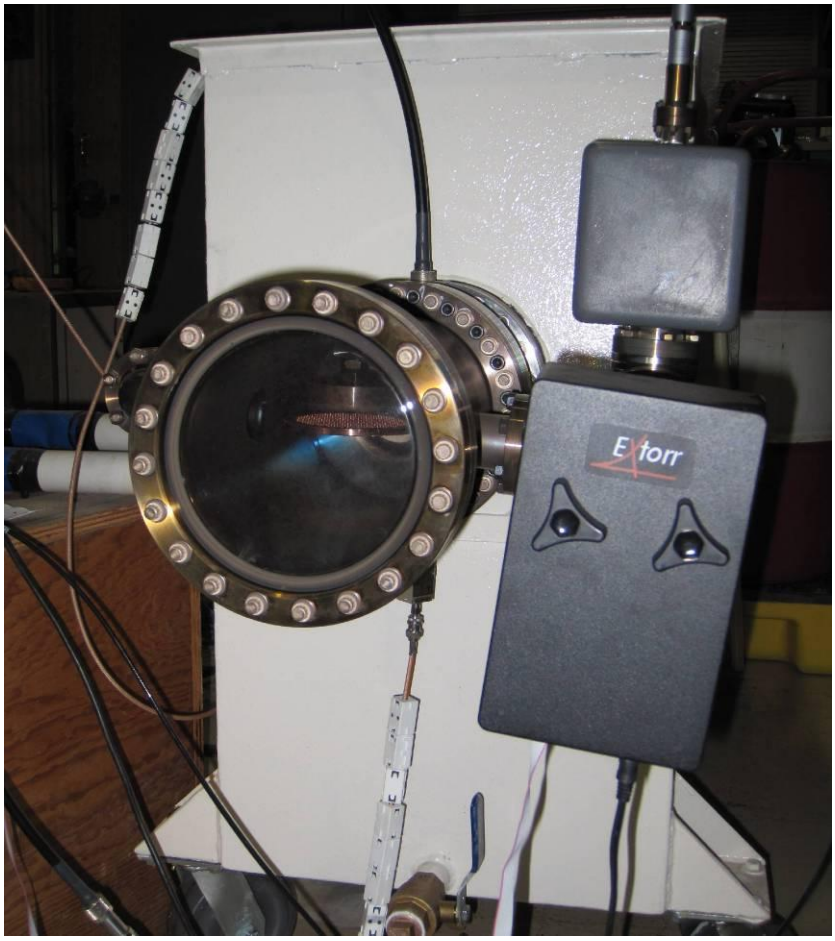

Figure 3.6: Vircator attached to Marx generator

Voltage and Current Diagnostics

The capacitive voltage probe is calibrated against a 5kV and all data is recorded by an *Agilent Infiniium* oscilloscope cable of 40 GSa/s and 12 GHz. Figure 3.7 shows the captured waveform of the 5kV pulse with the capacitive probe.

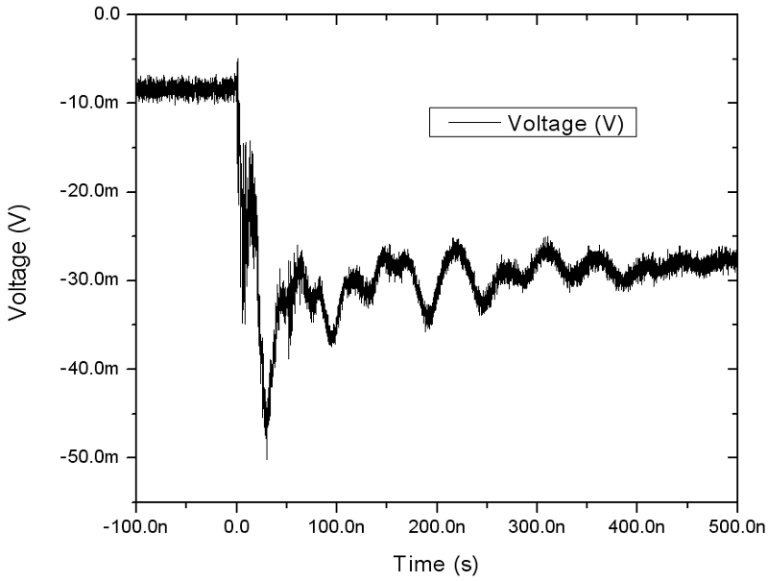

Figure 3.7: 5kV calibration shot

The model 101 Pearson coil was used to monitor current with a response of 0.005 V/A into a 50 Ω load. The Pearson coil sensitivity factor is specified from the manufacturer, so each current waveform has a scaling factor to be multiplied by. Figure 3.8 shows the captured current waveform for a shot with the vircator.

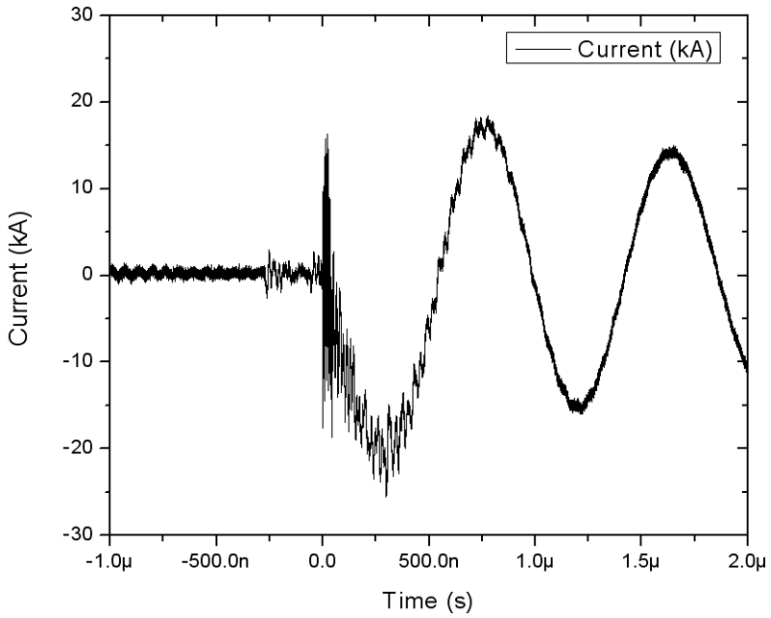

Figure 3.8: Current measurement using Pearson coil model 101

The usable rise time of the model 101 Pearson coil is listed as 100ns, therefore it is not fast enough to accurately monitor the current. Later, a Rogowski coil was used with the OFHC copper anode to get a more accurate current measurement.

CHAPTER IV

GAS EVOLUTION MEASUREMENTS

Multiple shots were taken with each anode. After each shot, the total pressure change and mass scans is recorded. The initial pressure is subtracted from the total pressure after the shot to obtain a difference in pressure. Using the Ideal Gas Law in Eq. 4.1, an approximate number of molecules evolved from operation of the vircator can be calculated.

$$PV=NkT \qquad [4.1]$$

From Eq. 4.1, P is the pressure of the system in Torr, V is the volume in Liters, N is the number of molecules, k is the Boltzmann's constant, and T is temperature in degrees Kelvin. The approximate number of molecules is calculated for each material. The calculated number of molecules is plotted per shot and presented on the same scale for each material, except Ta and OFHC copper. The scales for Ta and OFHC copper are twice as large due to their high outgassing characteristics. The lowest outgassing materials are compared later in the conclusion. Initial and post shot scans are shown for each material illustrating the residual gases found in the vacuum system. Analyzing the residual gases requires knowledge of the cracking patterns of certain gas species and knowing typical gases found in a vacuum system. Appendix A gives a detailed description of gas analysis with cracking patterns. Also with each shot, an effort was made to take a long exposure photograph of the vircator during operation. Pictures of each material are also presented with some corresponding voltage waveforms.

Stainless Steel

An initial RGA scan with a SS anode can be seen in Figure 4.1. Mass peaks can be seen for hydrogen (2 amu), methane (16, 15, and 14 amu), nitrogen (28 amu), carbon monoxide (28, 12 amu) and carbon dioxide (44 amu). A few smaller mass peaks can be seen at 17 and 18 amu, which indicate trace amounts of water in the vacuum system.

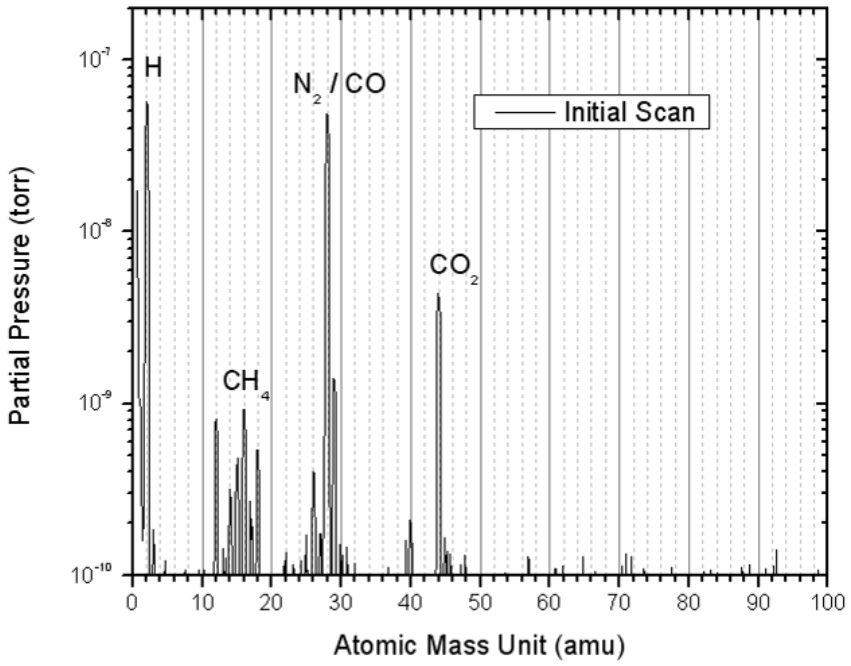

Figure 4.1: Initial RGA scan with SS anode

Before firing, a typical measured base pressure is in the ultra high vacuum range (~10^{-8} Torr). Then, the RGA's communications and control unit (CCU) is removed to prevent damage to its electrical components. Figure 4.2shows the last recorded RGA scan of an initial and post shot with the SS anode.

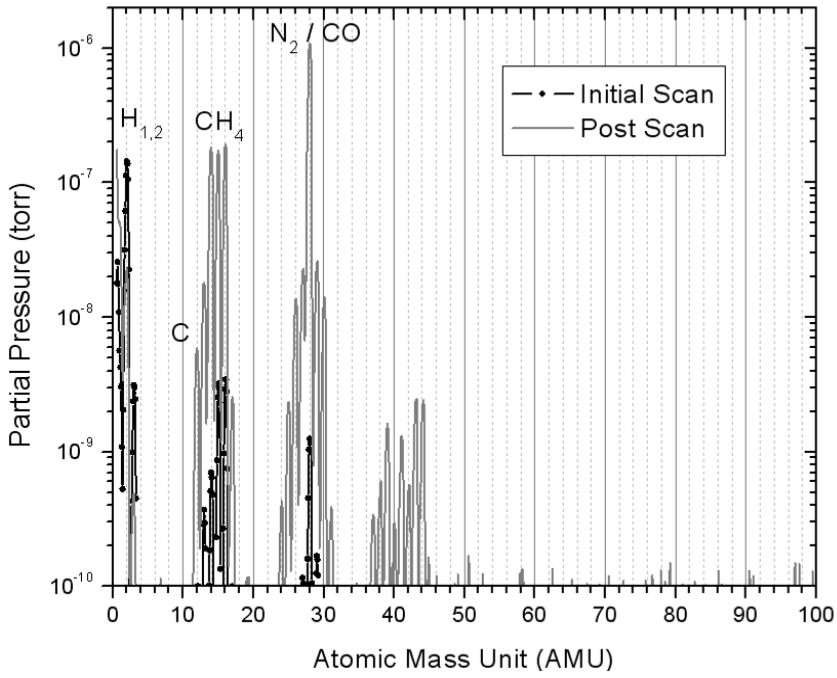

Figure 4.2: Last RGA scan with stainless steel anode

The post shot mass scan shows increases in partial pressures of all gases present in the system before the shot. Also noted is the increase in partial pressures in the range of 38 to 44 amu. 44 amu corresponds to carbon dioxide (CO_2) and the other mass peaks are groups of hydrocarbons. With the changes in total pressure, the approximate number of molecules is calculated for the SS anode and is show in Figure 4.3.

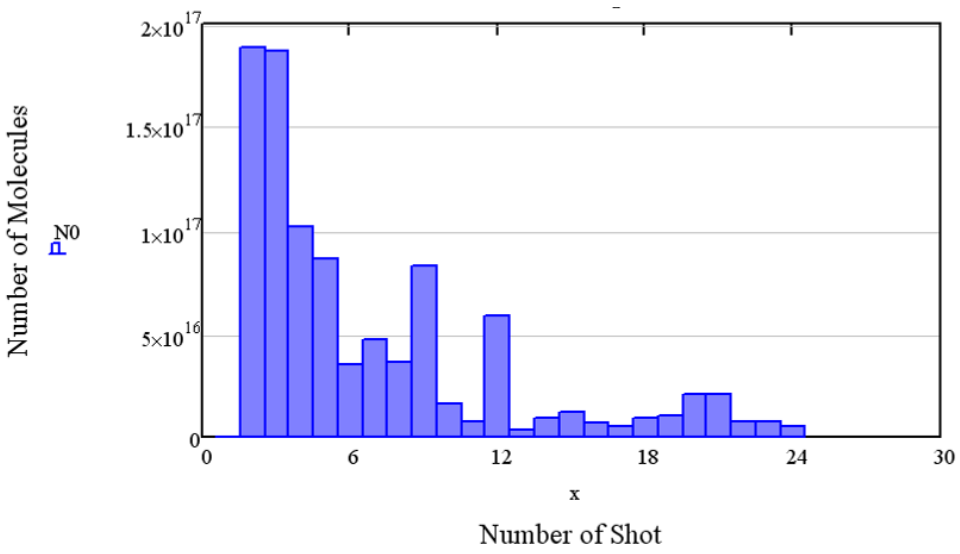

Figure 4.3: Approximate number of molecules evolved with SS anode

The trend seen in Figure 4.3 shows outgassing decreasing as the number of shots increases with the SS anode. The abnormal peaks at shots 9 and 12 could be attributed to the gap shorting resulting in increased outgassing due to high current density. Figure 4.4 shows a long exposure photograph with the stainless steel anode, during operation. The corresponding voltage waveform can be seen in Figure 4.5. Several photographs of the SS anode during operation are pictured in Figure 4.6.

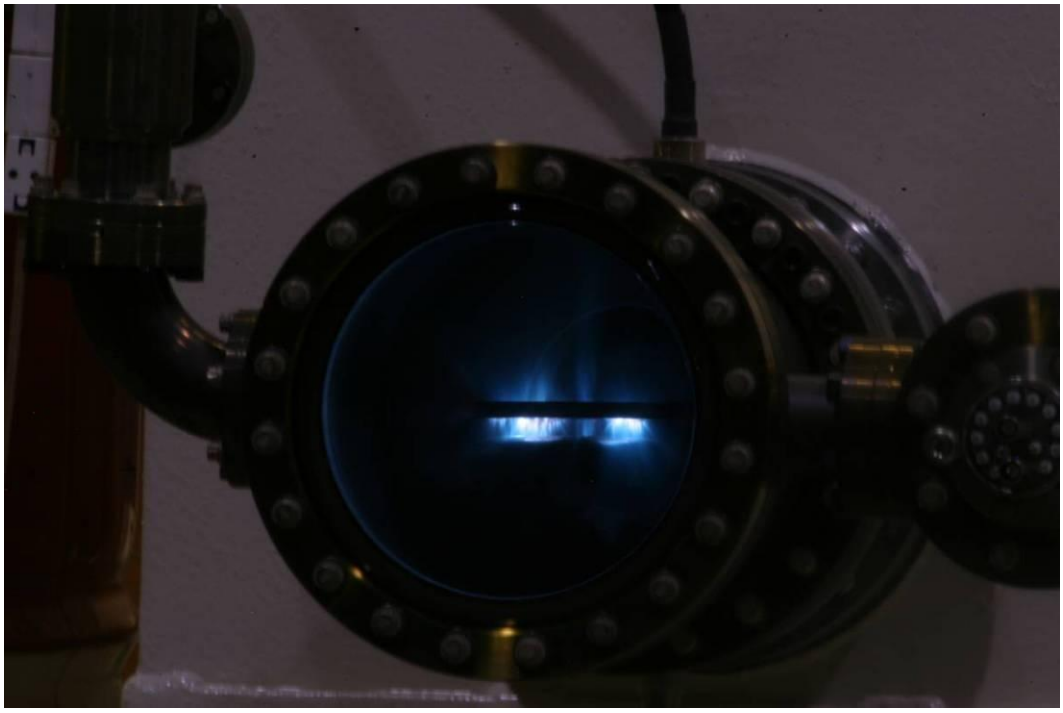

Figure 4.4: Long exposure photograph with SS anode

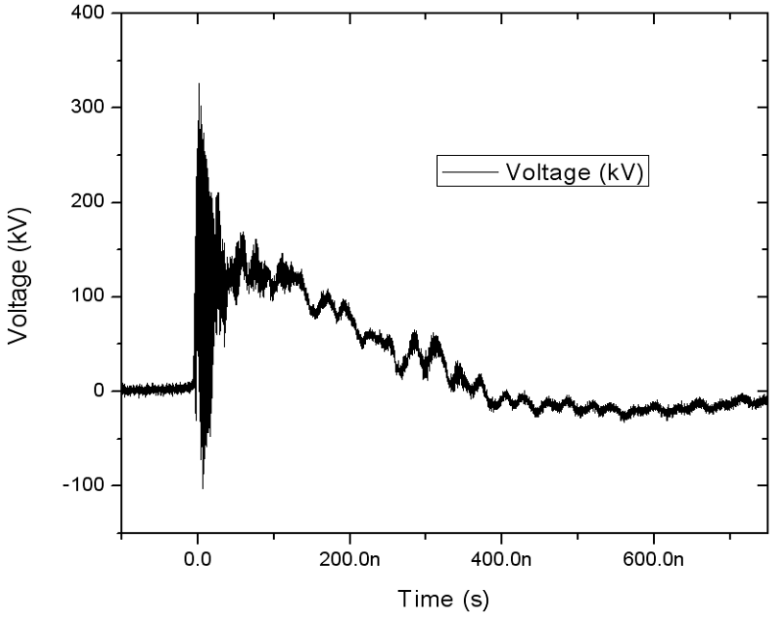

Figure 4.5: Voltage waveform for SS anode

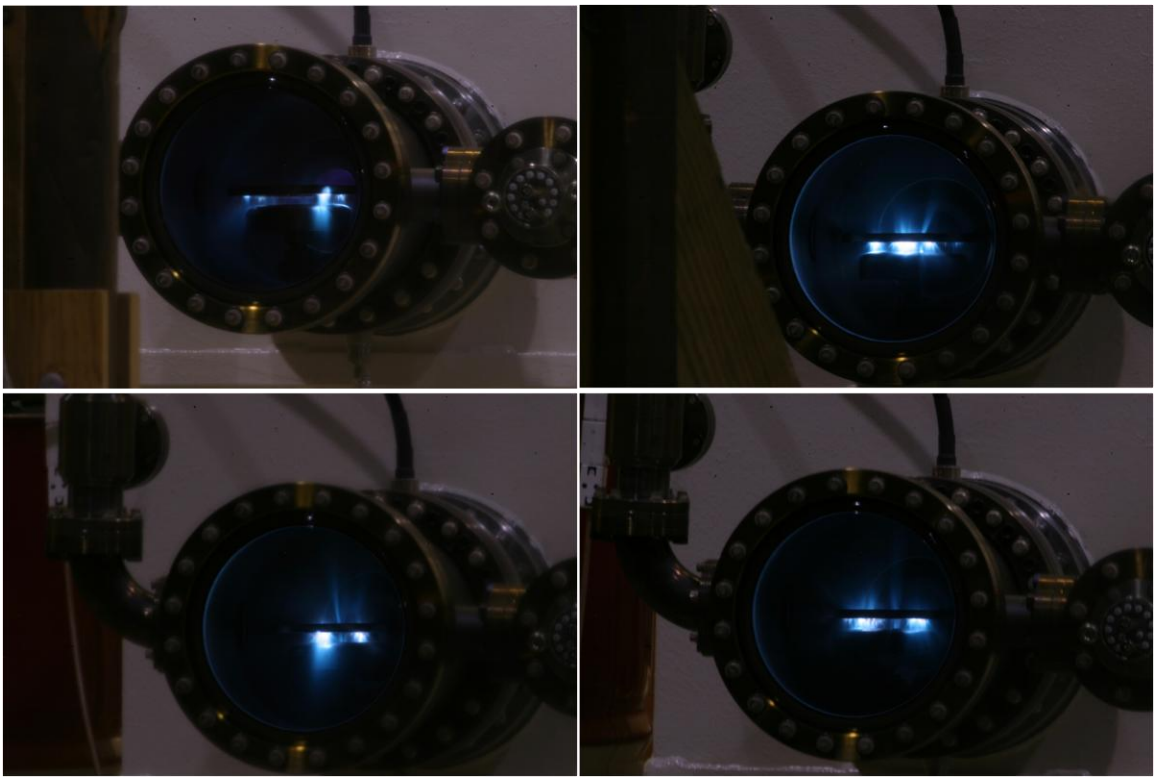

Figure 4.6: Several long exposure photographs with SS anode

Copper Tungsten

A copper alloy, consisting of 55% tungsten and 45% copper (CuW55), was chosen for its good electrical and thermal conductivity. Figure 4.7 shows an initial scan with the CuW55 anode with the 3 significant peaks corresponding to N_2 (28 amu), CO (also at 28 amu), H_2 (2 amu), and CO_2 (44 amu).

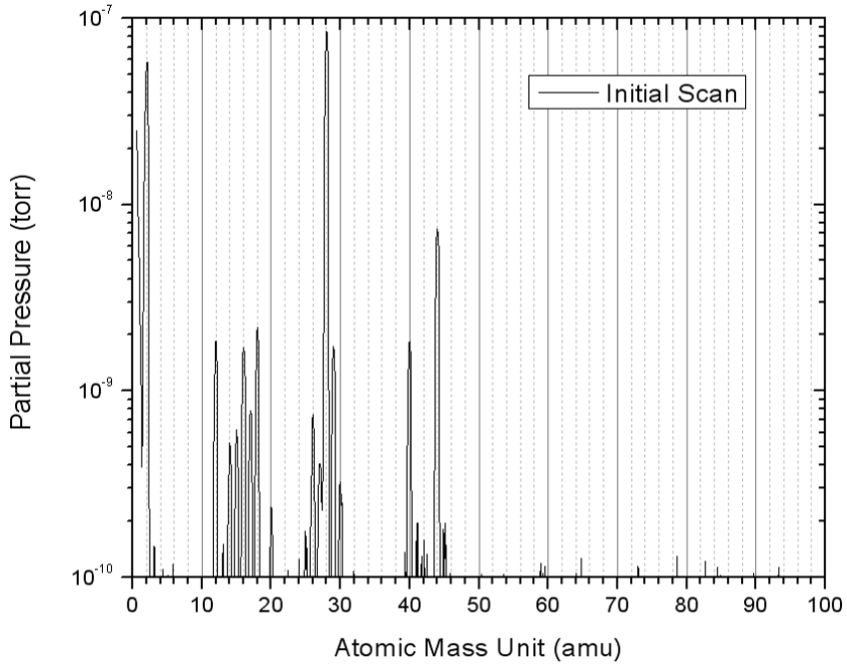

Figure 4.7: Initial RGA scan with CuW55

There are also smaller peaks for C (12 amu), CH_4 (16 amu) and Ar (40 amu). The absence of oxygen at 32 amu confirms that argon at 40 is just a residual gas and not an air leak. Figure 4.8 shows the post shot mass scan of the CuW55 anode.

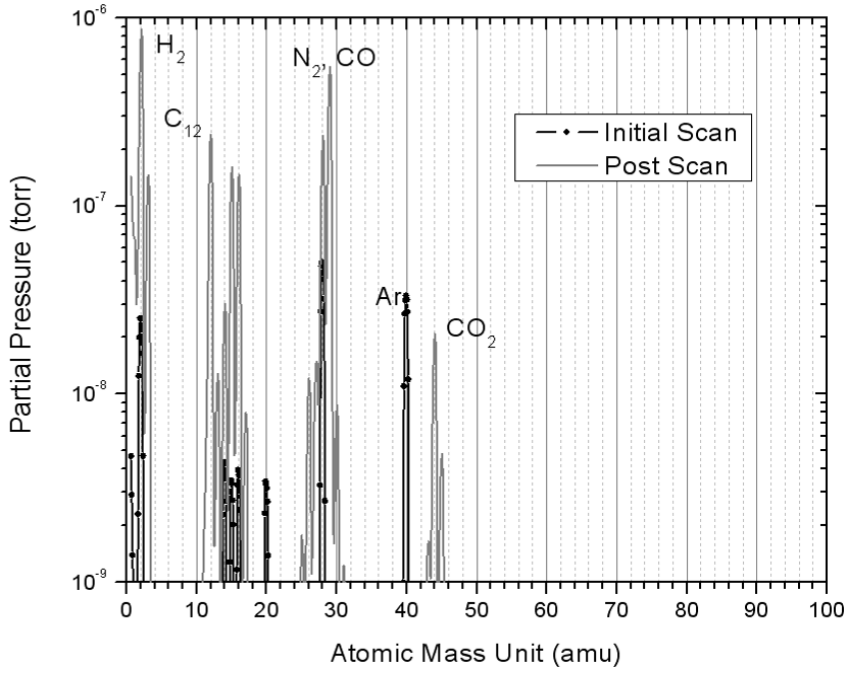

Figure 4.8: Last RGA scan with CuW55 anode

Partial pressure changes can be seen for all initial residual gases with the CuW55 anode. Given the total pressure changes with each shot of the CuW55 anode, the approximate number of molecules evolved from the surface is plotted in Figure 4.9.

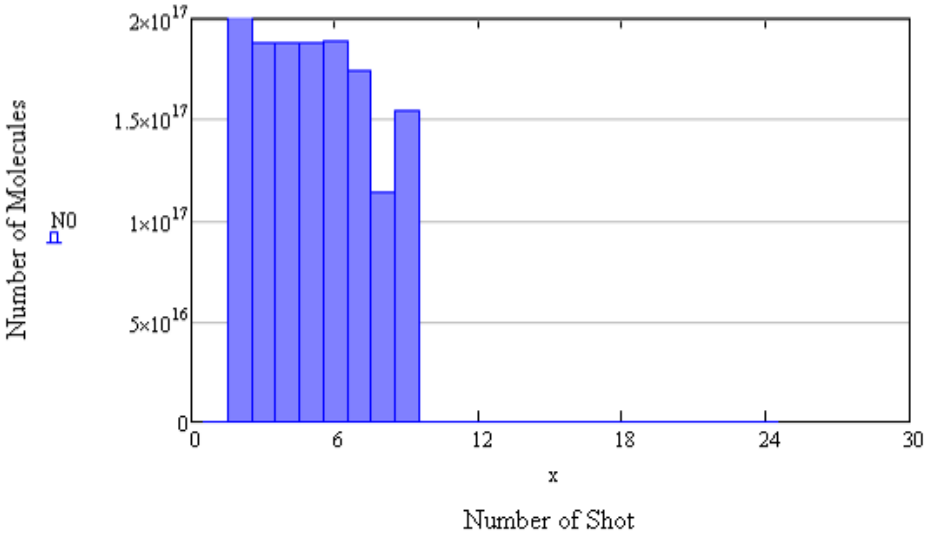

Figure 4.9: Approximate number of molecules evolved with CuW55 anode

It is evident that CuW55 outgases significantly more gas than SS. Figure 4.10 shows a long exposure photograph with the CuW55 anode. Between the A-K gap, the electron beam appears to be evenly distributed, but is too bright to be clearly determined. Figure 4.12 shows several photographs captured during the operation of the vircator with the CuW55 anode and each show similar details.

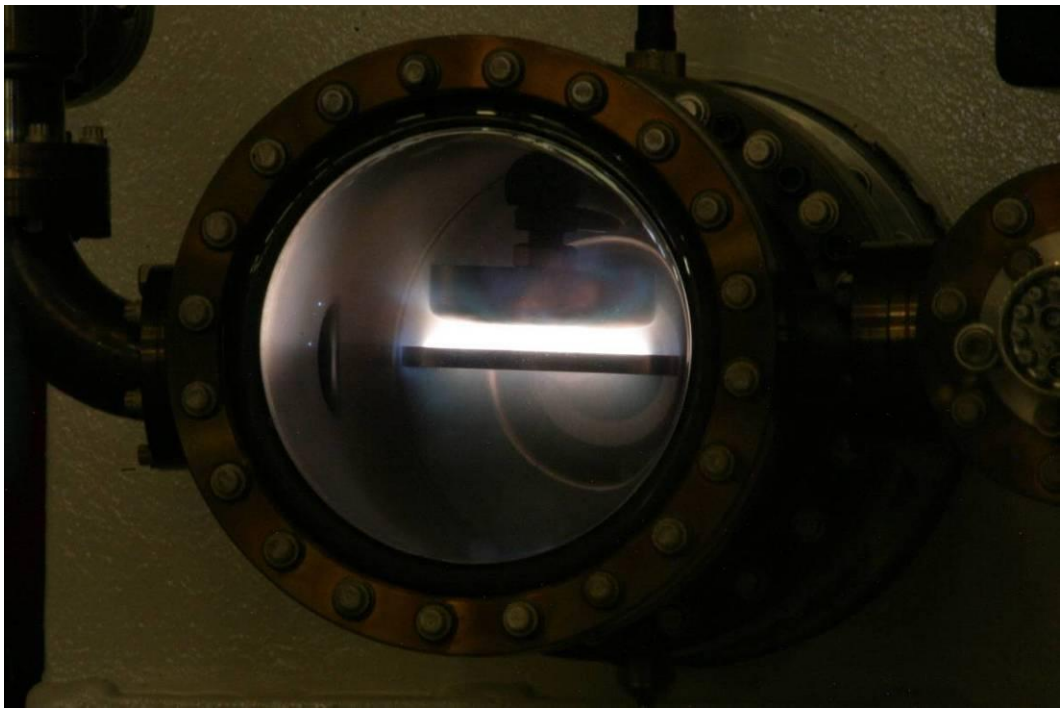

Figure 4.10: Long exposure photograph with CuW55 anode

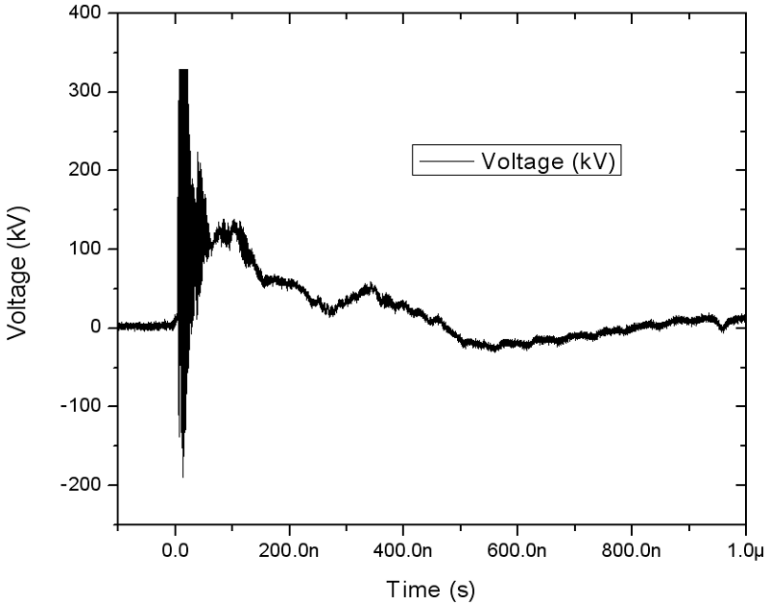

Figure 4.11: Voltage waveform for CuW55 anode

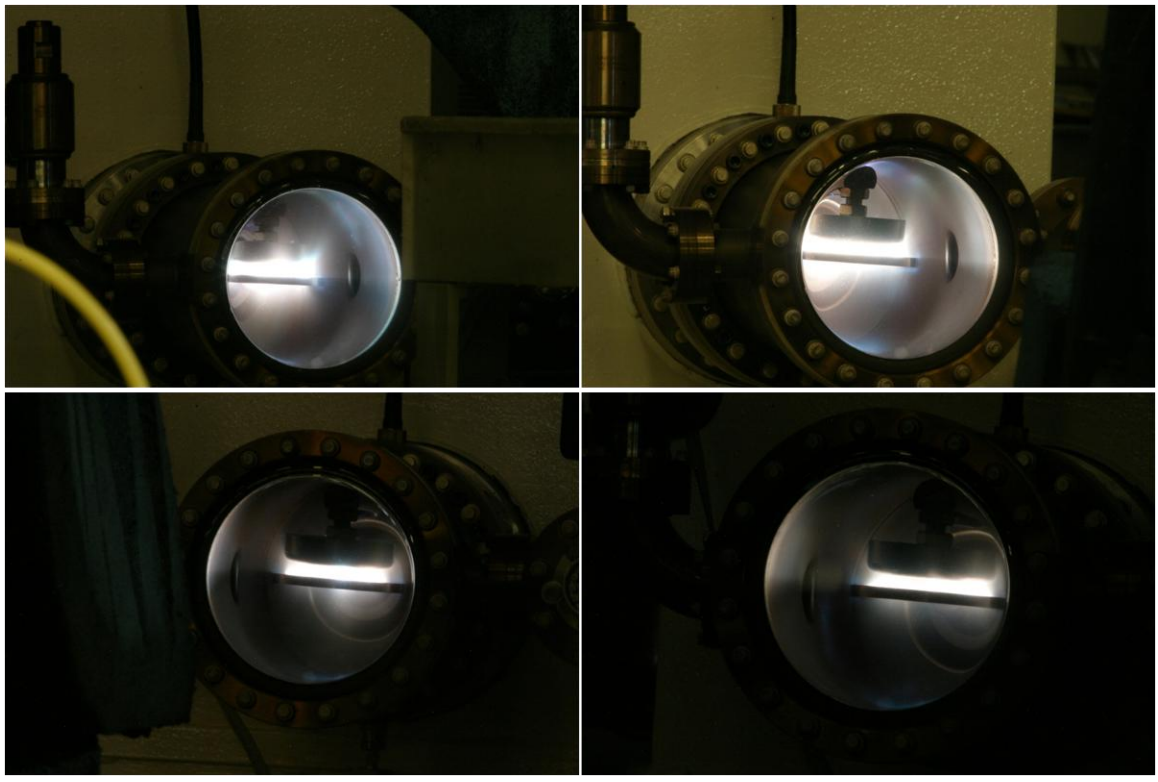

Figure 4.12: Several long exposure photographs with CuW55 anode

At the time of this writing, no further shots could be taken with the CuW55 anode due to breakdown of the high voltage feed through. Copper deposited on the surface of the ceramic feed through led to break down of the system.

Tantalum

A tantalum anode is selected due to its high melting point and resistance to corrosion. Residual gases seen in Figure 4.13 include H_2 (2 amu), CH_4 (16 amu), N_2, and CO (28 amu). Argon also appears but is several hundred times smaller than the H_2 peak.

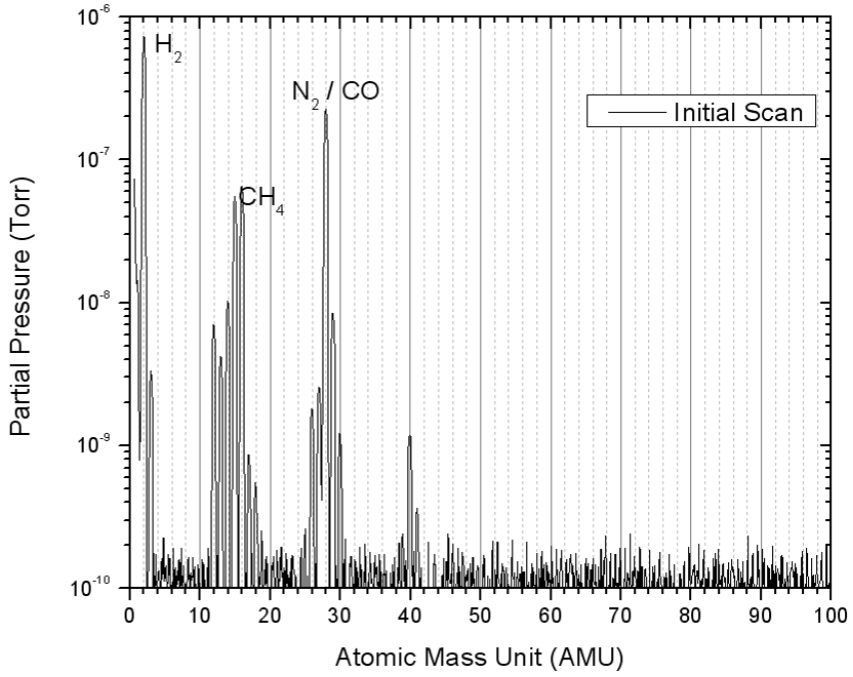

Figure 4.13: Initial RGA scan of with tantalum anode

The initial scan also reveals small traces of water vapor (H_2O) at 18 and 17 amu. The last RGA mass scan can be seen in Figure 4.14.

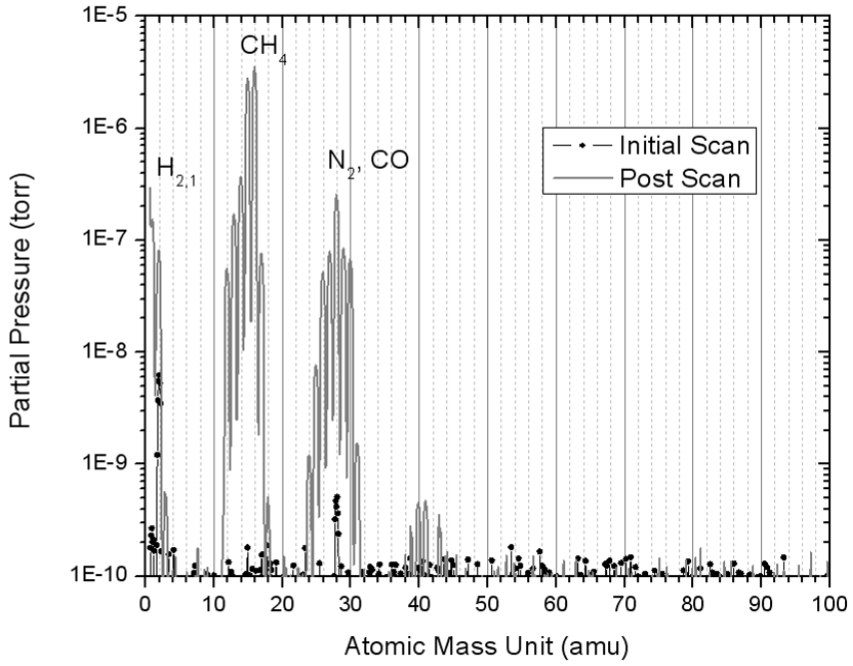

Figure 4.14: Last RGA scan with tantalum anode

The post scan with the tantalum anode exhibits the largest increase in partial pressure associated with CH_4. The pressure changes for each shot are used to obtain the number of molecules per shot graphed in Figure 4.15.

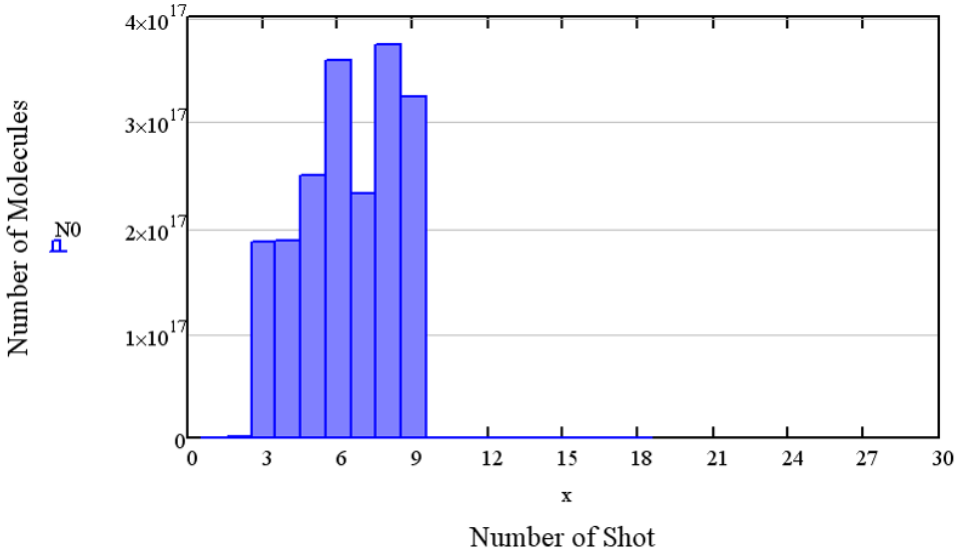

Figure 4.15: Approximate number of molecules evolved with tantalum anode

From the results seen in Figure 4.15, it appears that tantalum outgases erratically and does not show the desired decreasing trend. Figure 4.16 shows a long exposure photograph captured during operation of the vircator with the Ta anode. Trace lines, not detected previously with other material, can be seen indicating material is being driven off the surface of the anode. Figure 4.17 shows the typical voltage waveform for the Ta anode. Several long exposure photographs are grouped together and can be seen in Figure 4.18.

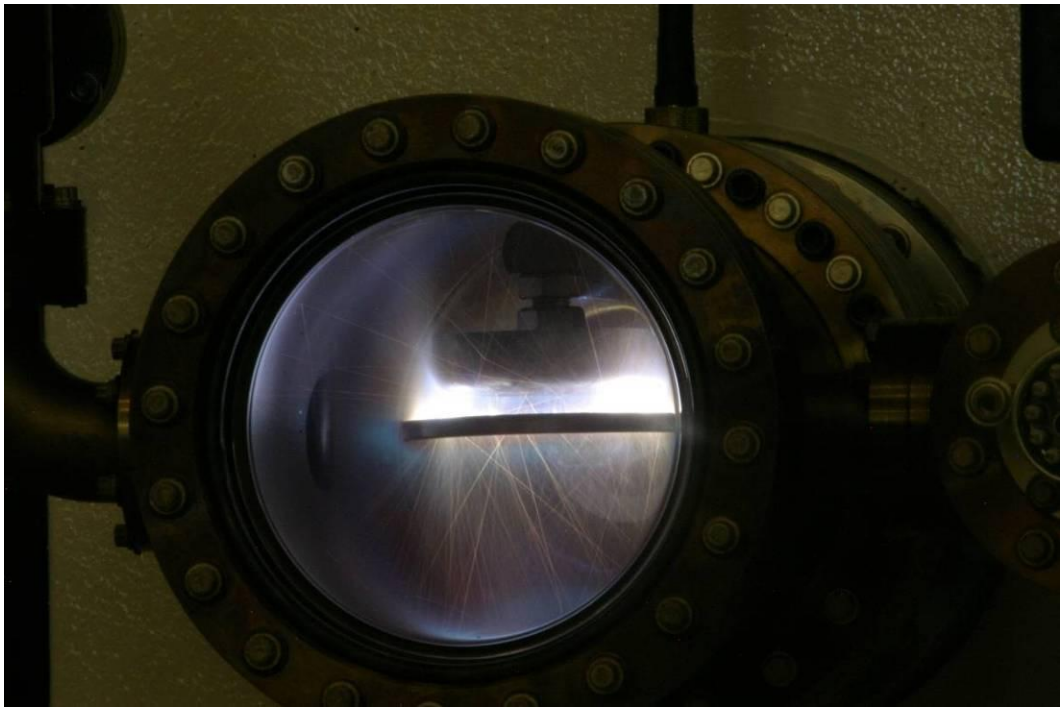

Figure 4.16: Long exposure photograph with Ta anode

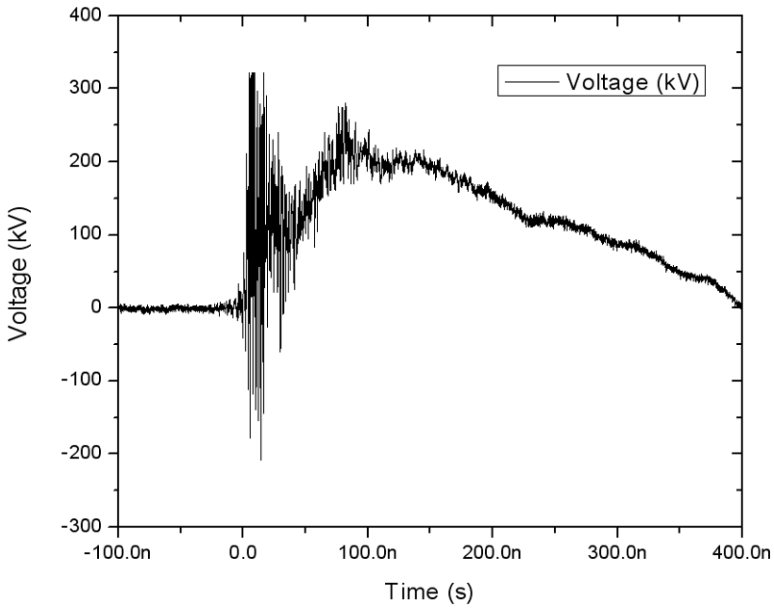

Figure 4.17: Voltage waveform with Ta anode

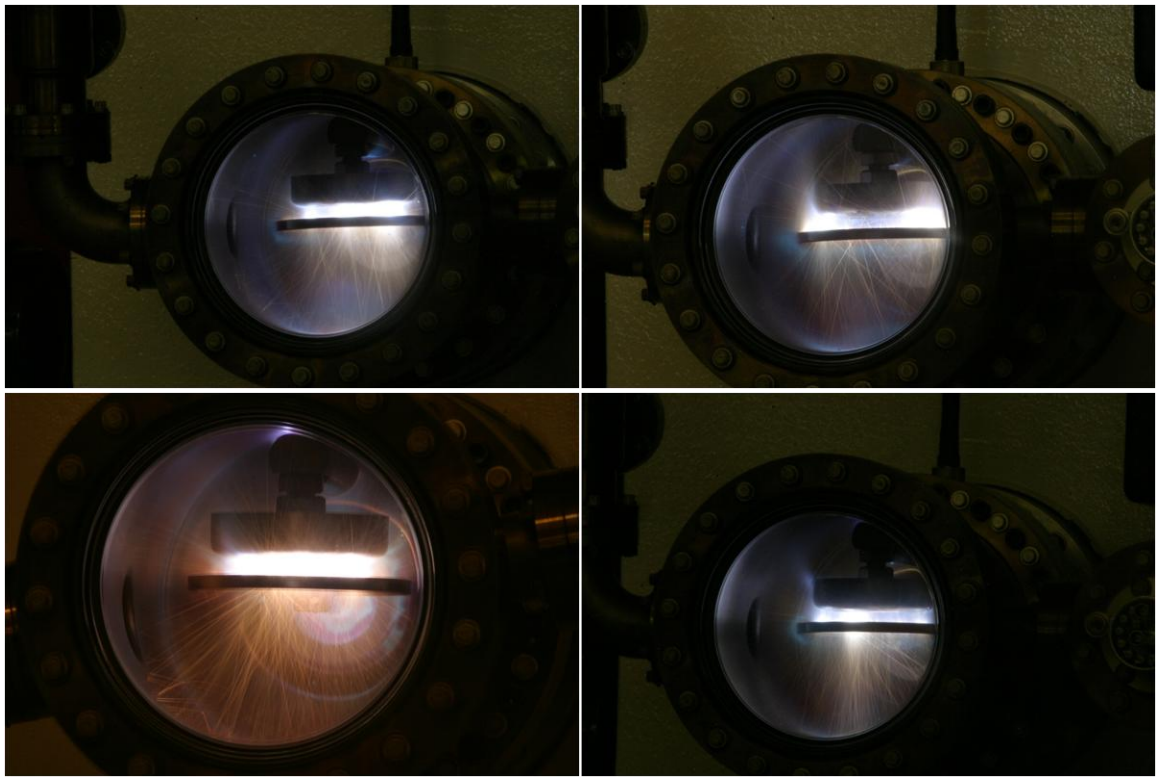

Figure 4.18: Several long exposure photographs with Ta anode

As seen in the bottom-left picture of Figure 4.18, break down of the high voltage ceramic feed through occurred. After removing the anode from the system, noticeable

damage to the Ta included pitting and roughness of the surface. Data for the Ta anode leads to conclude that Ta is not a suitable anode material for use in a vircator.

Nickel

A nickel 201(Ni) anode was tested in the vircator. The Ni used is 99% pure nickel and exhibits high electrical and thermal conductivities. Figure 4.19 shows the initial mass scan using the Ni anode inside the vircator.

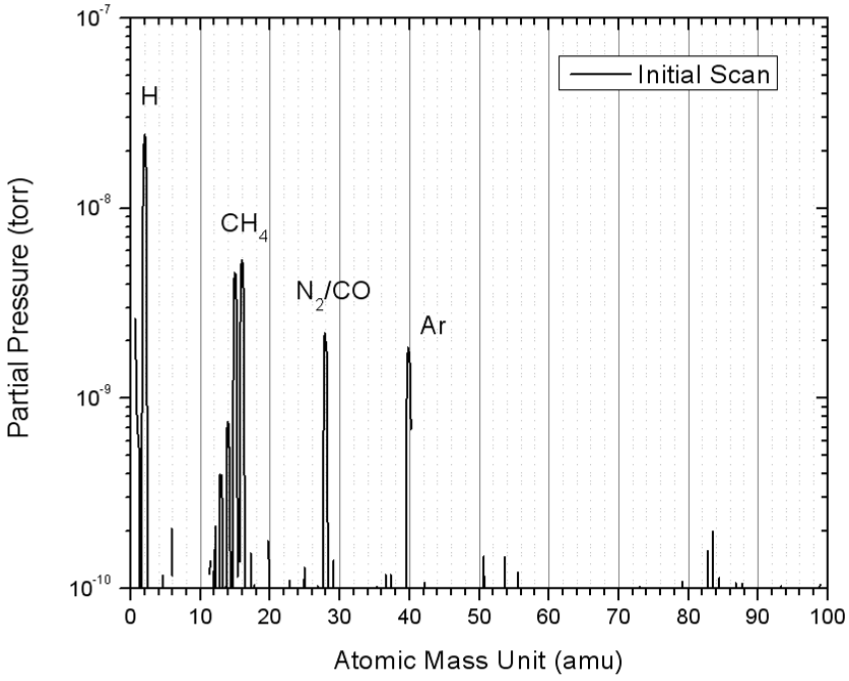

Figure 4.19: Initial RGA scan before first shot with nickel anode

Typical residual gases are found in the initial mass scan with hydrogen being the dominant gas. Figure 4.20 shows the initial and post scan with the nickel anode.

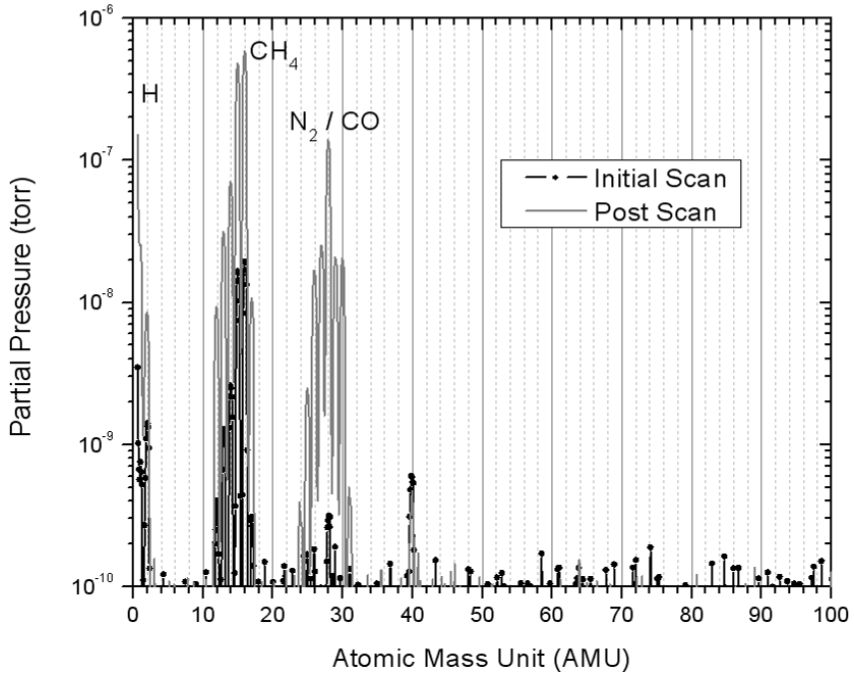

Figure 4.20: RGA scan of last recorded shot with nickel anode

With the nickel anode, the largest spike in partial pressure corresponds to 28 amu being a combination N_2 and CO based on cracking patters. Hydrocarbons are seen in the mid 20's and lower 30's amu. The molecular approximation of gases evolved can be seen in Figure 4.21.

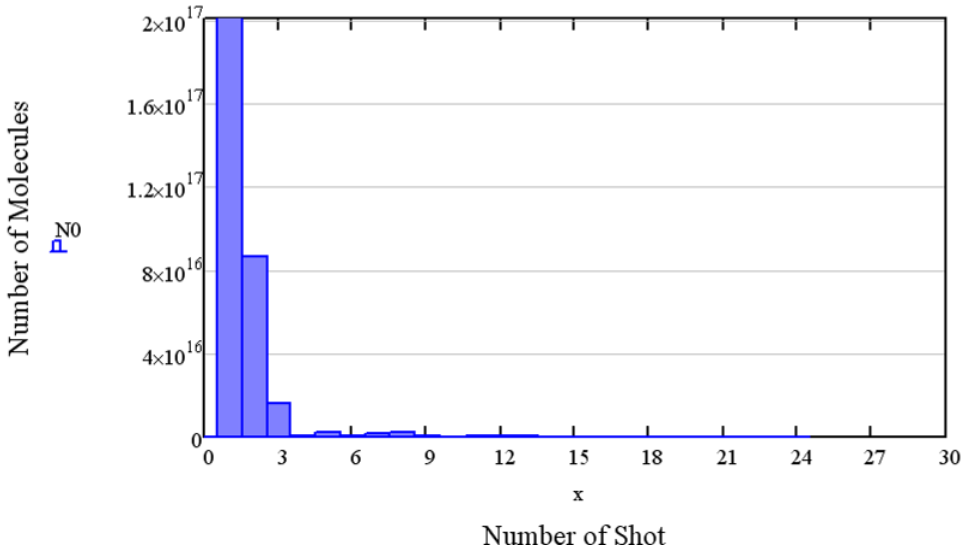

Figure 4.21: Approximate number of molecules evolved with nickel anode

After the 8th shot, the approximate number of molecules begins to level off and the same pressure is seen after each shot with little change. Figure 4.22 shows a photograph of the nickel anode during operation. The corresponding voltage waveform is seen in Figure 4.23.

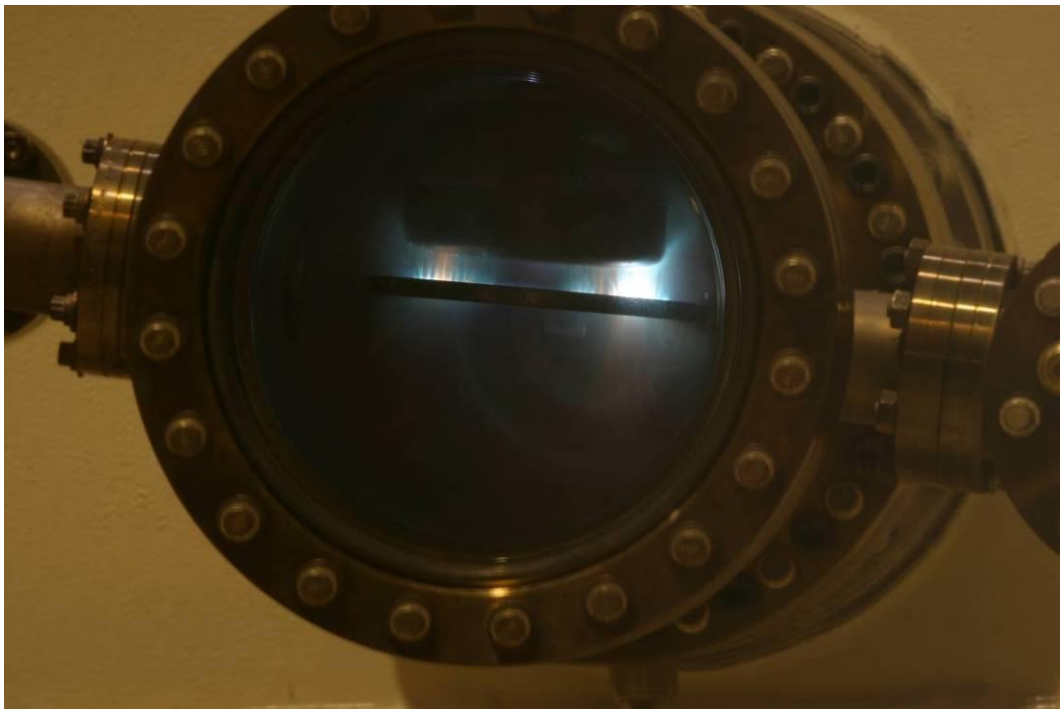

Figure 4.22: Long exposure photograph with nickel anode

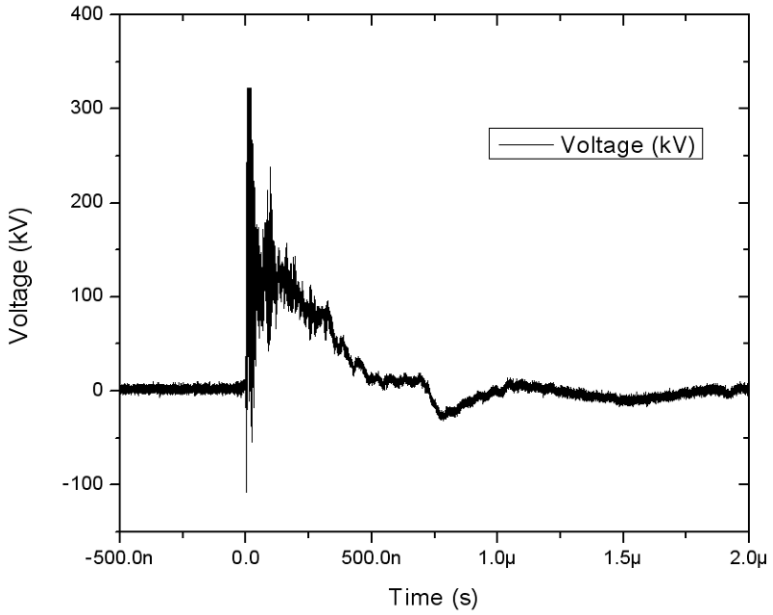

Figure 4.23: Voltage waveform for nickel anode

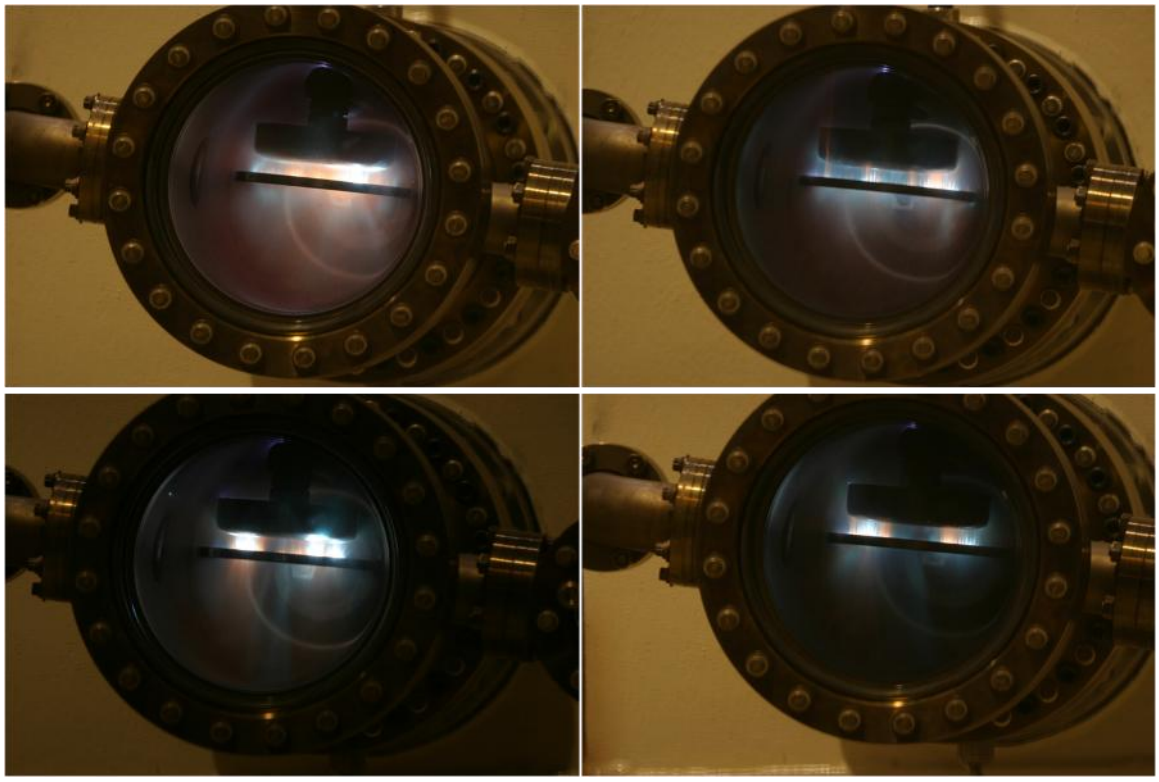

Figure 4.24: Typical long exposure photographs of nickel anode

The Ni anode displays a decrease in outgassing as the number of shots increases. Given the results from the previous anode materials, it was decided that an identical nickel anode would be machined and treated with a high temperature bake out under vacuum, not done previously. The nickel anode was baked at 800°C in a $1x10^{-7}$Torr vacuum oven. Figure 4.25 shows the initial RGA scan with the treated nickel anode and reveals peaks for H_2, CH_4, N_2, and CO as seen with the previous nickel anode. The initial scan also shows a decrease in the presence of argon in the vircator, giving the other gases higher partial pressure than the previous nickel anode. Figure 4.26 shows the post shot mass scan with the treated nickel anode.

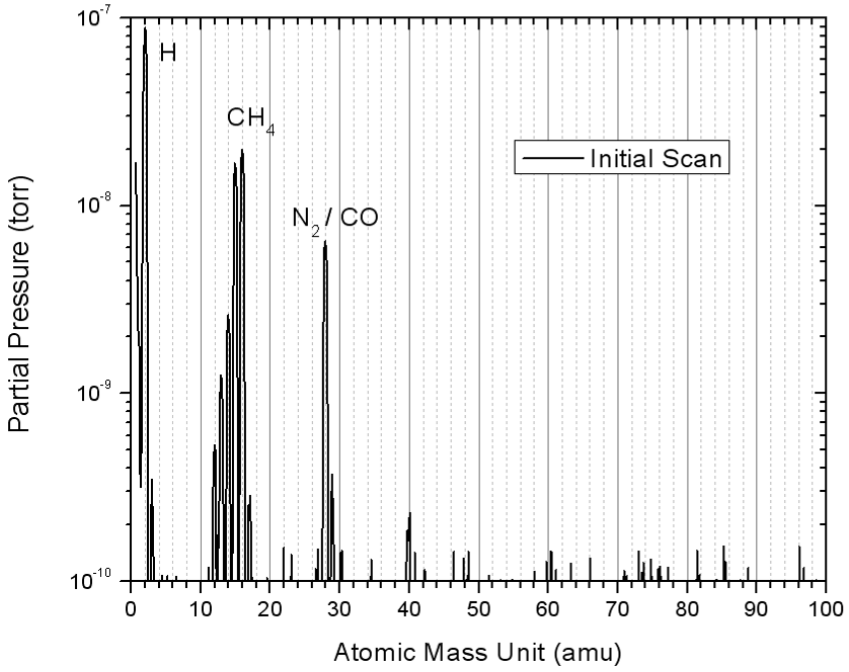

Figure 4.25: Initial RGA scan with treated nickel anode

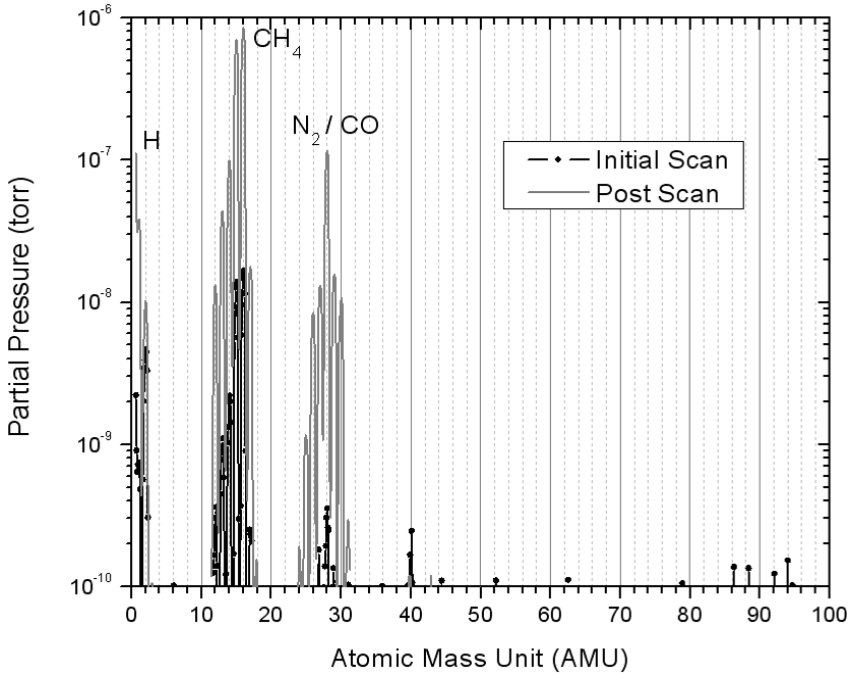

Figure 4.26: Last RGA scan with treated nickel anode

From Figure 4.26, the increase in partial pressures of the residual gases is similar to the previous nickel anode tested. The treated anode exhibits the largest increase in partial pressure to the mass peak at 28 and 16 amu, corresponding to N_2 and CH_4 respectively. The approximate number of molecules for the treated nickel anode is displayed in Figure 4.27 and compared to the previous nickel anode.

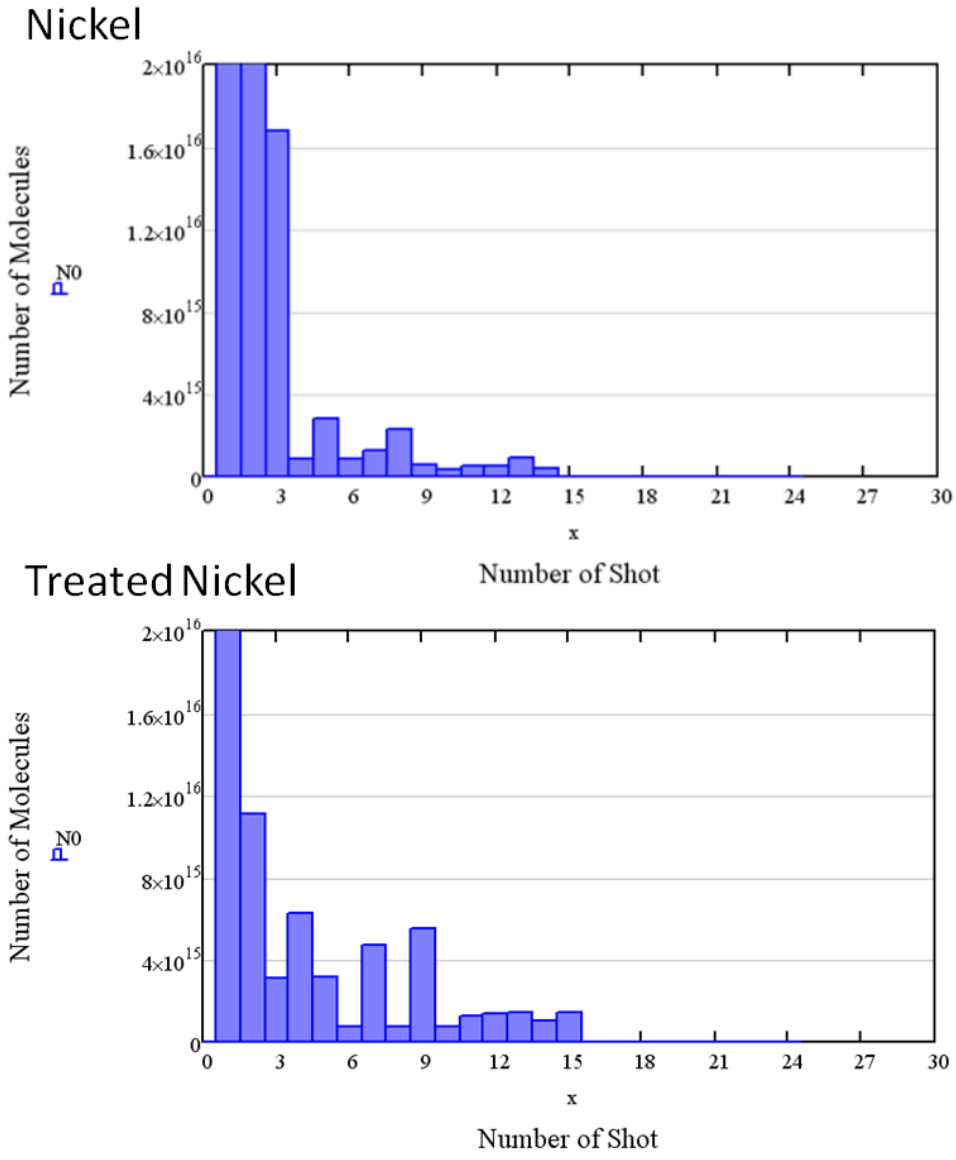

Figure 4.27: Approximate number of molecules evolved with the treated nickel anode

After shot number 9, the approximate number of molecules evolved per shot starts to level off and little change is seen. Figure 4.28 is a photograph of the treated nickel anode during operation followed by the corresponding waveform in Figure 4.29.

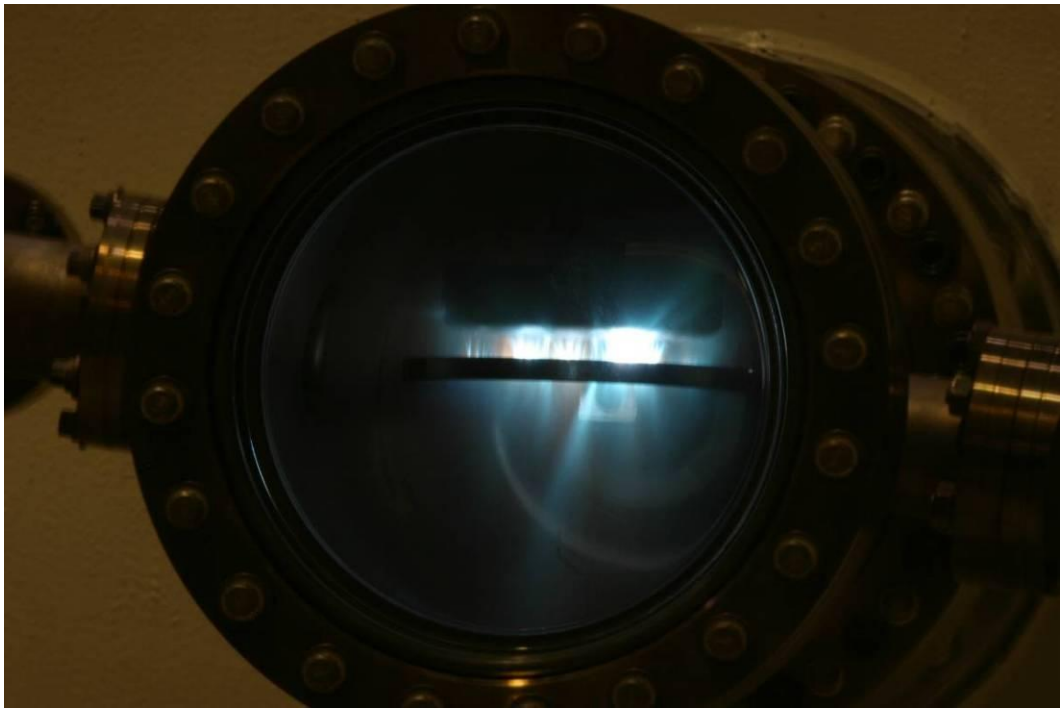

Figure 4.28: Long exposure shot with treated nickel anode

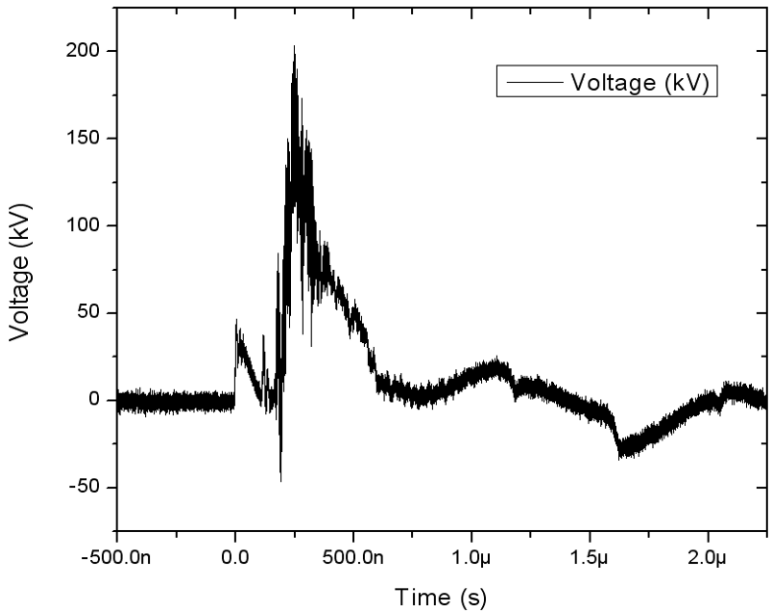

Figure 4.29: Voltage waveform for treated nickel anode

The voltage waveform in Figure 4.29 indicates an initial pre-firing from the Marx generator. This caused when the pressure in the spark gaps is insufficient to hold off the

40kV charging voltage. Adjustments were made to the spark gaps pressures and Figure 4.30 shows a typical waveform with the treated nickel anode.

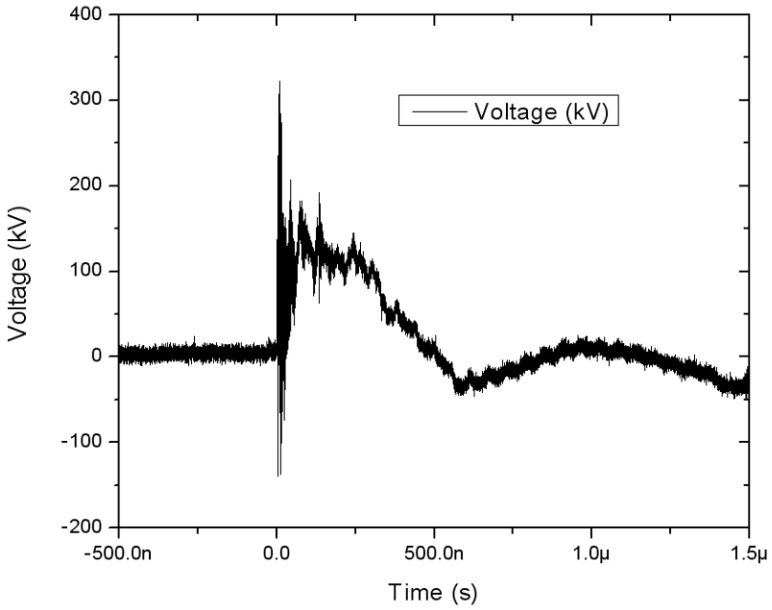

Figure 4.30: Typical voltage waveform with treated nickel anode

Figure 4.31 shows several photographs of the treated nickel anode during operation. The first picture captured is seen in the upper-left corner. Continuing in a clock-wise direction, the bottom-left picture is the last picture captured with the treated nickel anode.

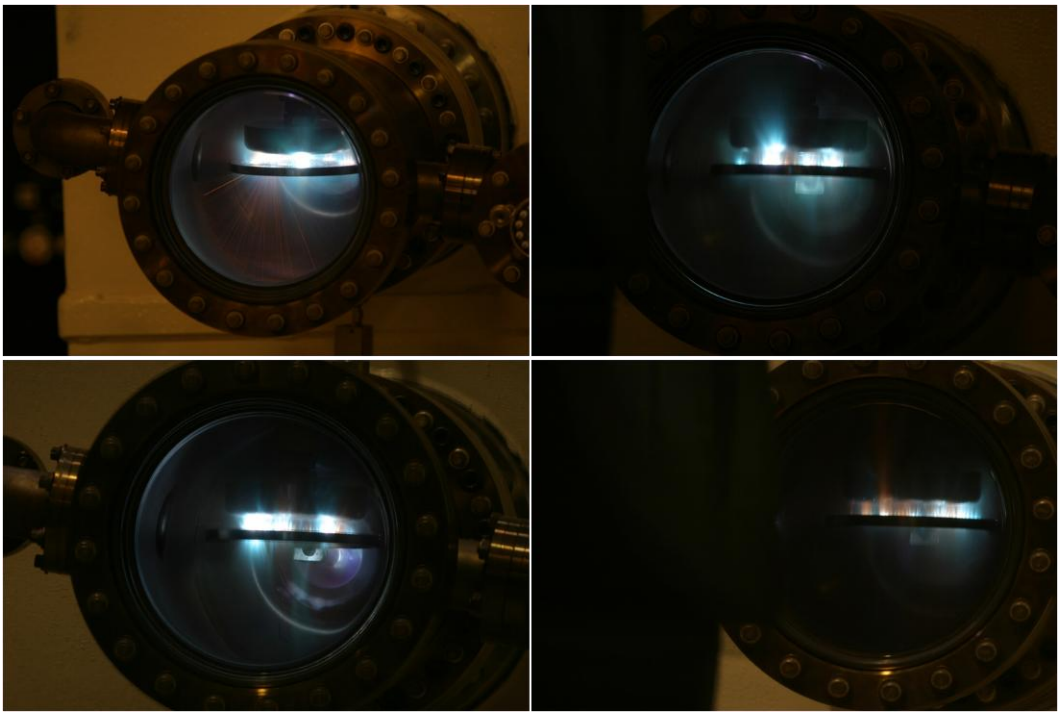

Figure 4.31: Long exposure photographs with treated nickel anode

In the last picture, breakdown of the ceramic feed-through can be seen. The data from the treated (Figure 4.27) and un-treated (Figure 4.21) nickel anodes reveals that the high temperature bake under vacuum helps to minimize the initial outgassing, when firing in the vircator.

Molybdenum

Molybdenum (Mo) was used for a material in the vircator for its high melting point and good electrical conductivity. Figure 4.32 is the initial mass scan for Mo and reveals typical residual gases seen previously in testing other materials.

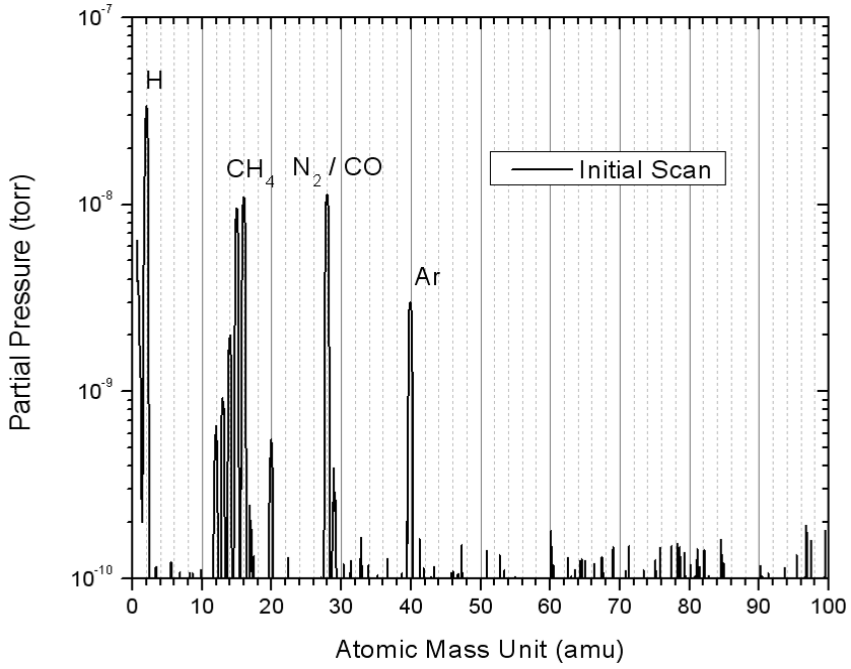

Figure 4.32: Initial RGA scan with a molybdenum anode

For Mo, the largest mass peaks correspond to H_2, CH_4, N_2, CO, and Ar. Figure 4.33 shows the last RGA scan with Mo anode before and after firing.

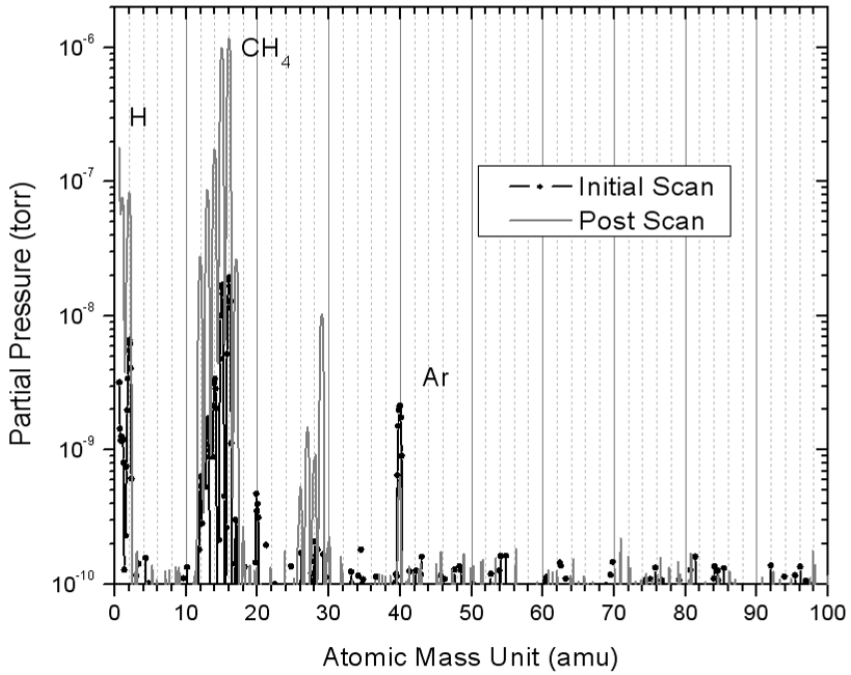

Figure 4.33: Last RGA scan with molybdenum anode

For the Mo anode, the largest partial pressure increase is for CH_4. The peak at mass 29 amu is associated with the hydrocarbons left in the system. The approximate number of molecules evolved per shot is seen in Figure 4.34 and shows a slightly higher, but similar outgassing trend to nickel.

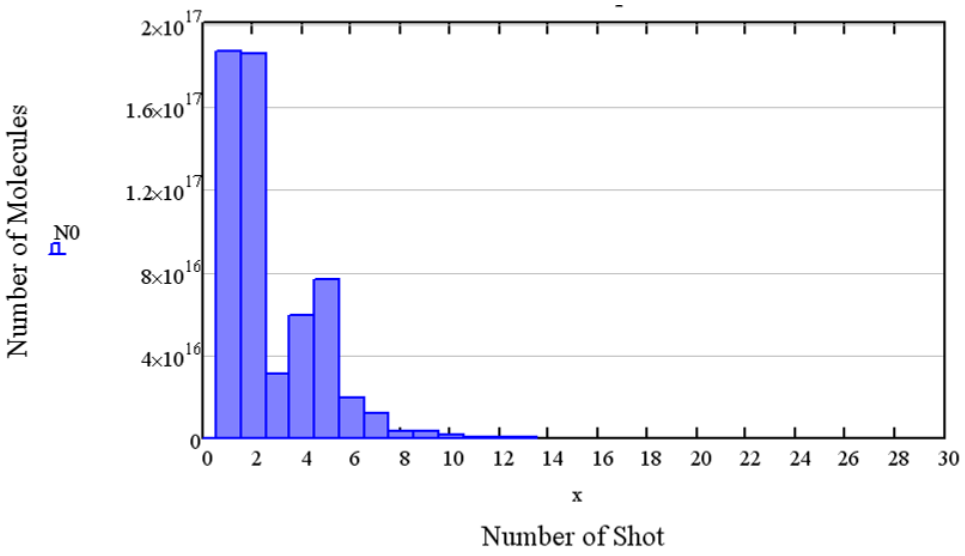

Figure 4.34: Approximate number of molecules per shot with molybdenum anode

Figure 4.35 shows a photograph captured with the Mo anode. As with the Ta anode, trace lines can be seen where material is being driven off the anode surface. Figure 4.36 shows the typical voltage waveform with the Mo anode.

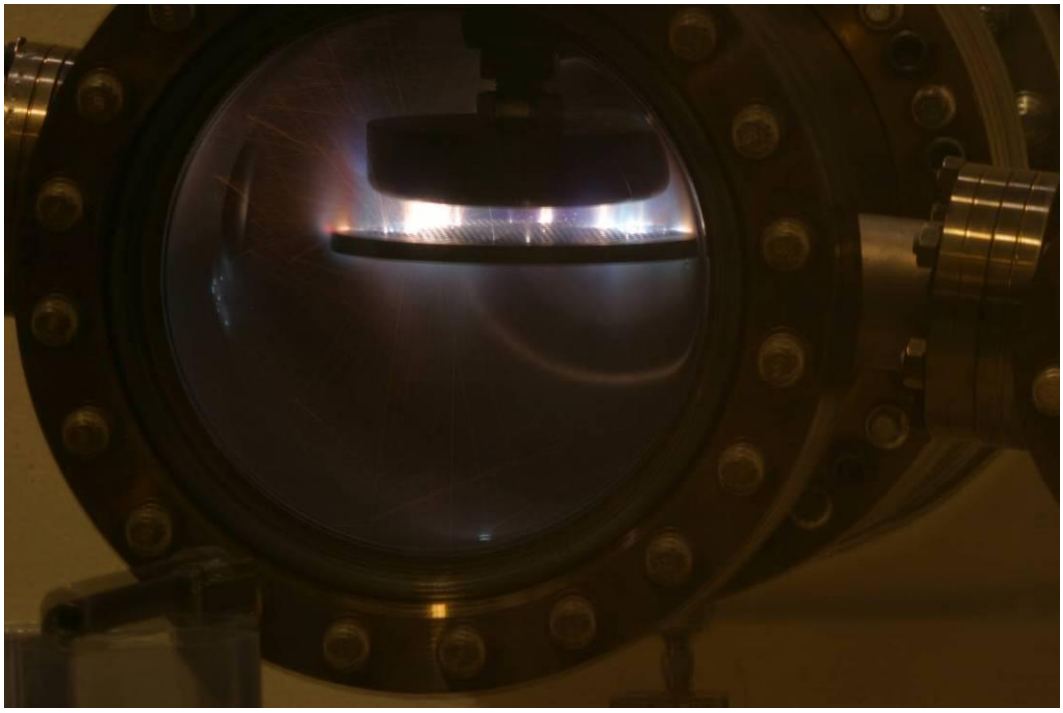

Figure 4.35: Long exposure photograph with Mo anode

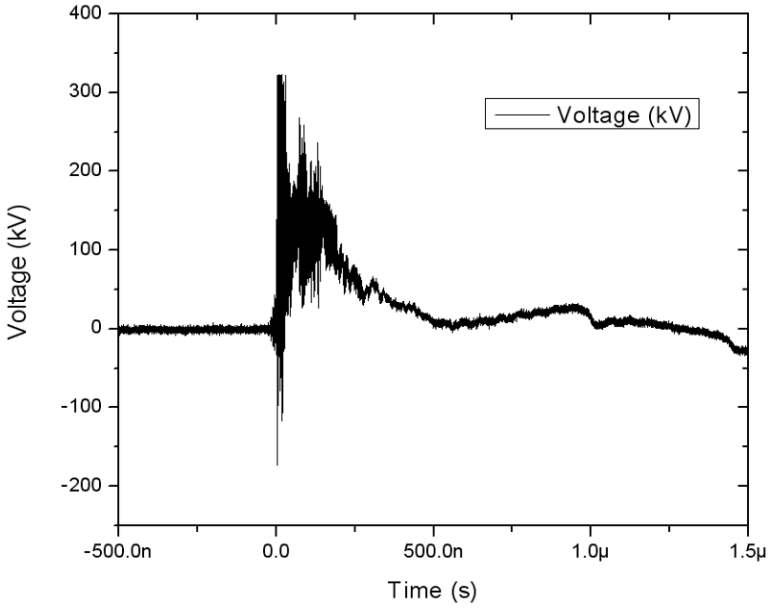

Figure 4.36: Voltage waveform for Mo anode

OFHC Copper

Oxygen-free high-conductivity copper, which is 99.99% copper, is the last material tested for use as an anode inside the vircator. The high thermal and electrical conductivity are favorable characteristics for use as an anode. Figure 4.37 shows an initial scan of the OFHC copper anode.

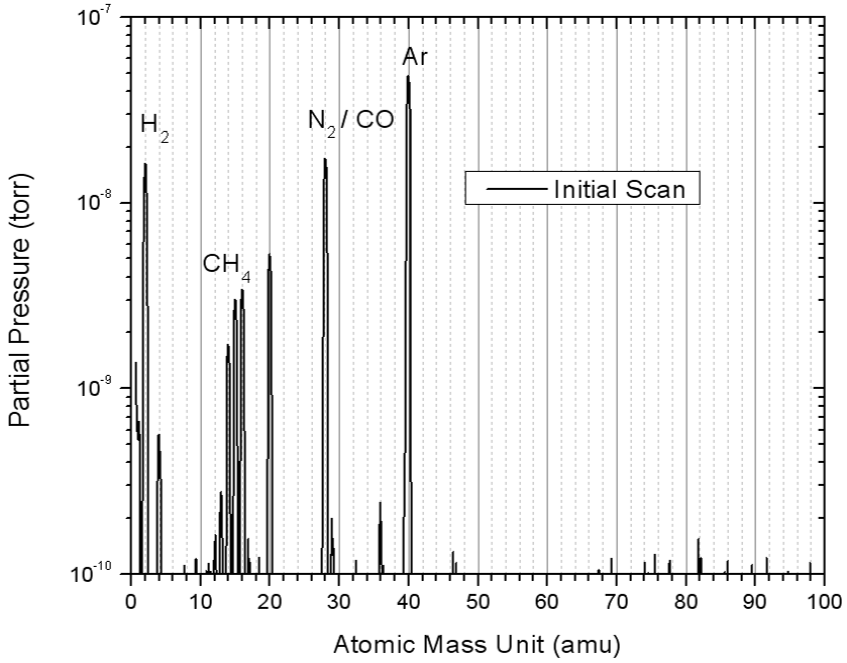

Figure 4.37: Initial scan with OFHC copper anode

The large peak at 40 amu is associated with argon and its cracking pattern confirms that with the peak at 20 amu. It is also noted that the vircator system took several days to reach a baseline pressure in the ~10^{-8} Torr. A mass scan was taken with the electron multiplier (EM) on and is shown in Figure 4.38.

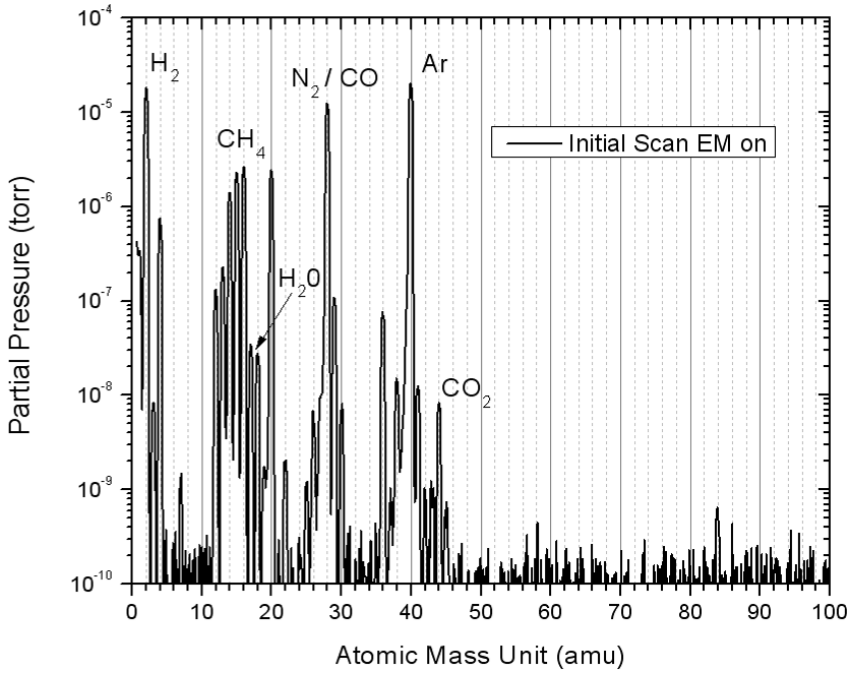

Figure 4.38: Initial scan with electron multiplier (EM) on

With the EM on, the mass scan reveals trace amounts of water vapor (H_2O) and other contaminants. The presence of water vapor and contaminants explains why the vircator needed to be pumped longer to achieve a desirable vacuum quality. Figure 4.39 shows the post shot mass scan with partial pressure increases in all residual gases, except Ar. This could mean that Ar is a residual gas and is not evolved from the surface of the anode material during vircator operation. Also, the post shot mass scan shows increases in partial pressures from contaminants see only previously with the EM on in Figure 4.38. At this time, only three complete mass scans were taken with the OFHC copper anode and Figure 4.40 shows a graph for the approximate number of molecules evolved from the material. Note that the scale is on the same order as the Ta anode, and the approximations for OFHC copper indicate that it outgases significantly during operation.

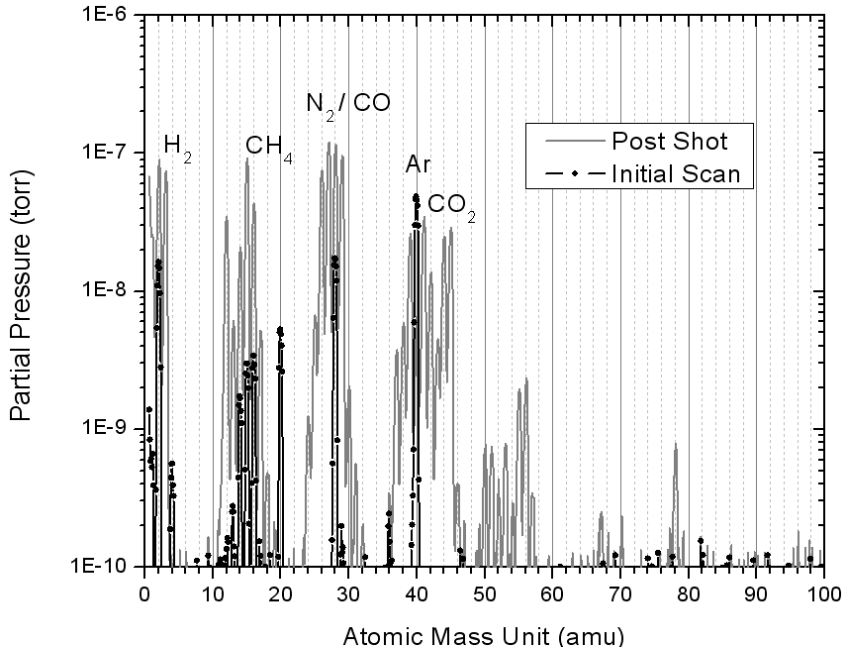

Figure 4.39: Post scan with OFHC copper anode

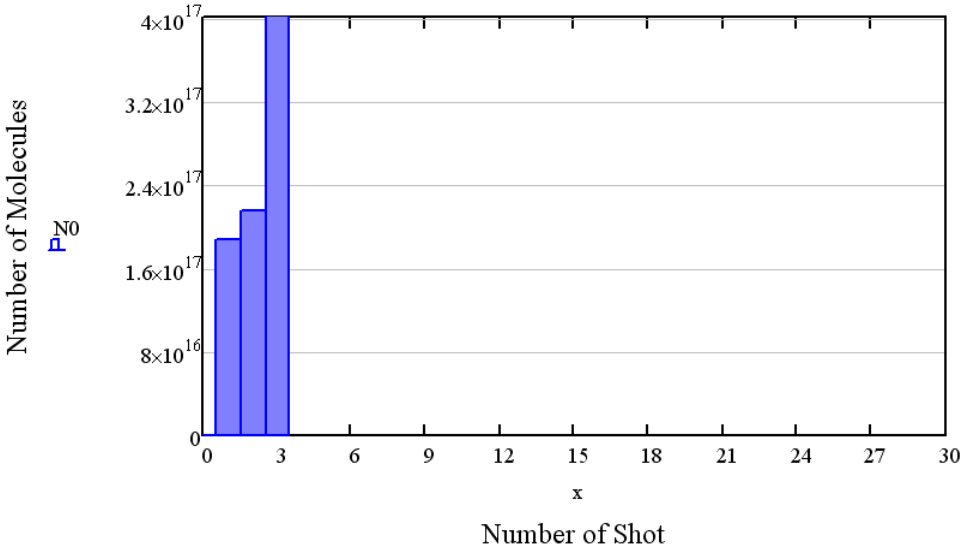

Figure 4.40: Approximate number of molecules evolved with the OFHC copper anode

A long exposure photograph was captured with the second shot with the OFHC copper anode and can be seen in Figure .41. Here break down of the ceramic high voltage feed through can already be seen. A third shot also revealed breakdown of the

ceramic high voltage feed through, so a complete system break down of the OFHC copper anode was done.

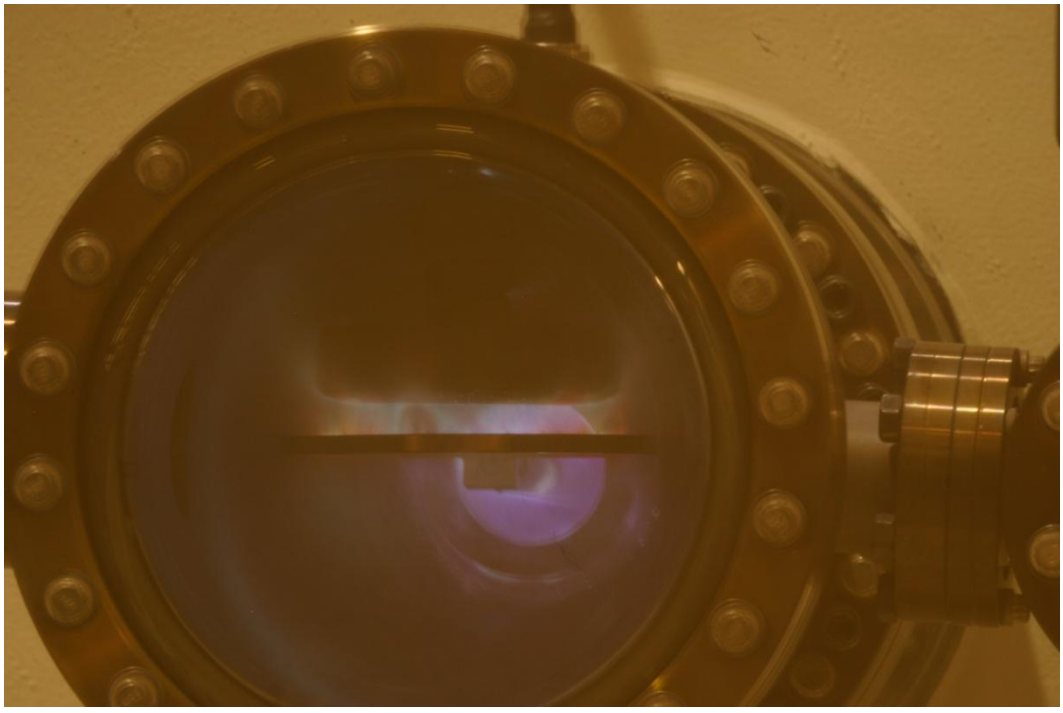

Figure 4.41: Long exposure photograph with OFHC copper anode

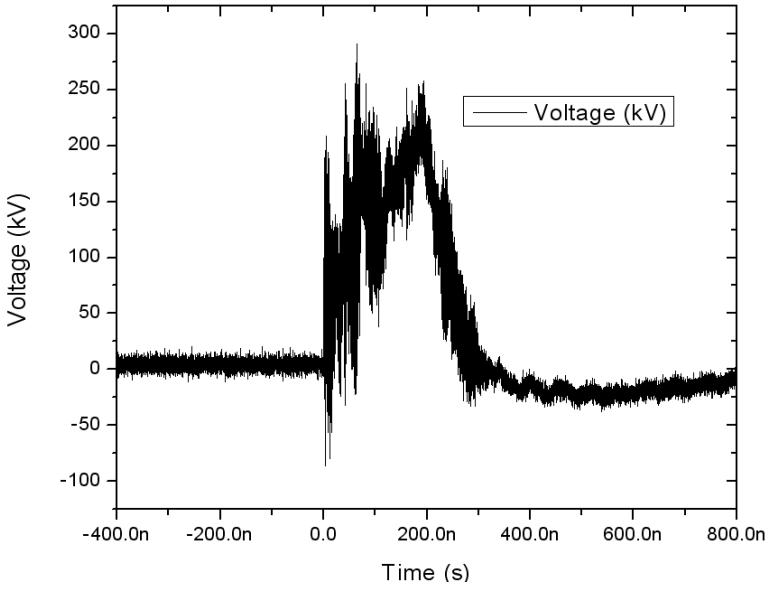

Figure 4.42: Voltage waveform for OFHC copper anode

Figure 4.43 reveals that copper is deposited on the surface of the cathode and stainless steel vacuum walls. Also seen in Figure 4.43 are spots left behind from possible contaminants in the vircator. Break down and copper being deposited on the surfaces inside the vircator led to end the use of OFHC copper as an anode material.

Figure 4.43: Copper deposits on the cathode and SS tube

Conclusion

Residual gas measurements have been utilized to characterize gases evolved during the operation of a vircator using different anode materials. Typical residual gases

found include hydrogen, nitrogen, carbon monoxide, and argon. Pressure changes for each material were recorded showing initial spikes in partial pressures for the first few shots for each material. Table 4.1 shows pressure changes of specific gases for each material tested.

Table 4.1: Table of Pressure Changes for Specific Gases

Material	H2	N2 / CO	CH4	CO2	Ar
Stainless Steel	2.14E-06	4.87E-07	3.81E-07	5.97E-09	1.54E-09
Copper Tungsten	5.61E-07	2.43E-07	1.00E-07	5.81E-08	7.01E-09
Tantalum	7.43E-08	2.57E-07	3.18E-06	1.48E-10	3.38E-10
Nickel	7.08E-09	1.33E-07	5.52E-07	5.37E-11	7.00E-11
Treated Nickel	5.52E-09	1.15E-07	8.34E-07	3.19E-11	-1.28E-10
Molybdenum	7.69E-08	7.20E-10	1.13E-06	7.20E-10	-1.53E-09
OFHC Copper	1.03E-05	8.37E-07	6.12E-07	1.39E-07	-5.05E-08

The nickel anodes show the smallest pressure changes for each specific gas when compared to the other materials. The nickel anode, treated with a high temperature bake out under vacuum, indicates it helps minimize initial outgassing in the material. The largest pressure change for the treated nickel anode is 1.15×10^{-7} Torr corresponding to a combination of N_2 and CO. Figure 4.44 shows a comparison of the number of molecules evolved for the two nickel and molybdenum anodes.

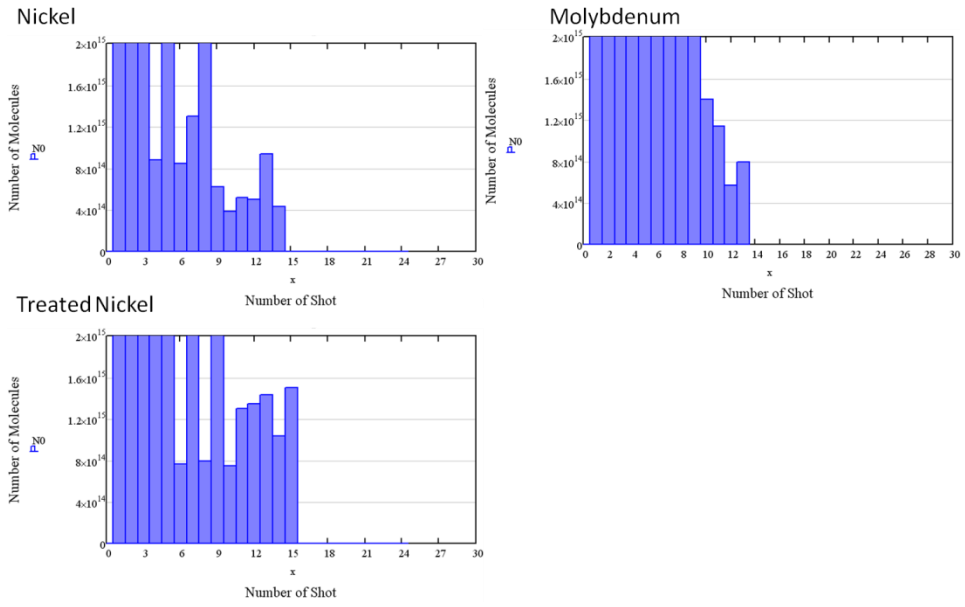

Figure 4.44: Comparison of molecular approximation of Ni and Mo anodes

For the nickel anodes, the outgassing trends appear similar as the number of shots increases. This confirms that the high temperature bake out under vacuum only helped to minimize initial outgassing. Further treatments to the nickel anode could be done to further improve its outgassing characteristics. Molybdenum showed a desirable trend in outgassing, but is limited by the number of shots taken. Future testing with the molybdenum anode could be to investigate the outgassing trend with treatments to the anode material. Further investigation into feed through design could also help to minimize the occurrence of breakdown seen during testing. The work presented here will lead to further improvements in the vircator design. As materials that outgas the least are further tested, a suitable anode will be used for maximum performance of the vircator.

REFERENCES

[1] J. Benford, J. A. Swegle, and E. Schamiloglu, *High Power Microwaves*, 2nd Ed. New York: Taylor & Francis, 2007.

[2] V.D. Selemir, A. E. Dubinov, B. G. Ptitsyn, A. A. Evseenko, V. A. Letyagin, R. K. Nurgaliev, V. G. Suvorov, and A. V. Sudovtsov, "The influence of vacuum conditions on the microwave generation in a vircator," Technical Physical Letters. vol. 27, no. 11. pp 967-968, November 2001.

[3] R. J. Umstattd, C. A. Schlise, F. Wang, "Gas evolution during operation of a CsI-coated carbon fiber cathode in a closed vacuum system," IEEE Trans. on Plasma Science. Vol. 33, No. 2, pp. 901-910, April 2005.

[4] M. Litz, D. Judy, G. Huttlin, C. Lazard, "Gases evolved from the common cold cathode," in *Proc. of the SPIE Intense Microwave Pulses IV*, vol. 2843, pp. 90-95, August 1996.

[5] Y. Chen, J. Mankowski, J. Walter, M. Kristiansen, and R. Gale, "Cathode and anode optimization in a virtual cathode oscillator," IEEE Trans. On Dielectrics and Electrical Insulation. vol. 14, no. 4, pp. 1037-1044, August 2007.

[6] J. Walter, J. Dickens, M. Kristiansen, "Performance of a compact triode vircator and Marx generator system, *Pulsed Power Conference*, 2009. *PPC '09. IEEE*, vol., no., pp. 133-137, June 28 2009-July 2 2009.

[7] International Bureau of Weights and Measures, *The International System of Units (SI)* (8th ed.), p. 126, ISBN 92-822-2213-6 (2006).

[8] M. Lara, "Reflex-Triode Geometry of the Virtual Cathode Oscillator," M.S. thesis, Texas Tech University, Lubbock, TX, United States, 2003.

[9] *Extorr XT Series RGA Manual*, Rev. 090629, Extorr Inc., New Kensington, PA, 2009.

[10] Extorr Inc. (2006, July 17). *Residual Gas Analyzer Principles of Operation* [Online]. Available: http://www.extorr.com/residual_gas_analyzer.htm

[11] MatWeb, "Material Property Data," [Online]. Available: www.matweb.com. [Accessed Jan. 2011].

APPENDIX A

ANALYSIS OF RESIDUAL GASES IN A VACUUM SYSTEM

Many typical gases undergo fragmentation or cracking when they are ionized. A molecule's cracking pattern is what helps to easily identify typical gas species under vacuum. Take the mass sweep seen in Figure A.1.

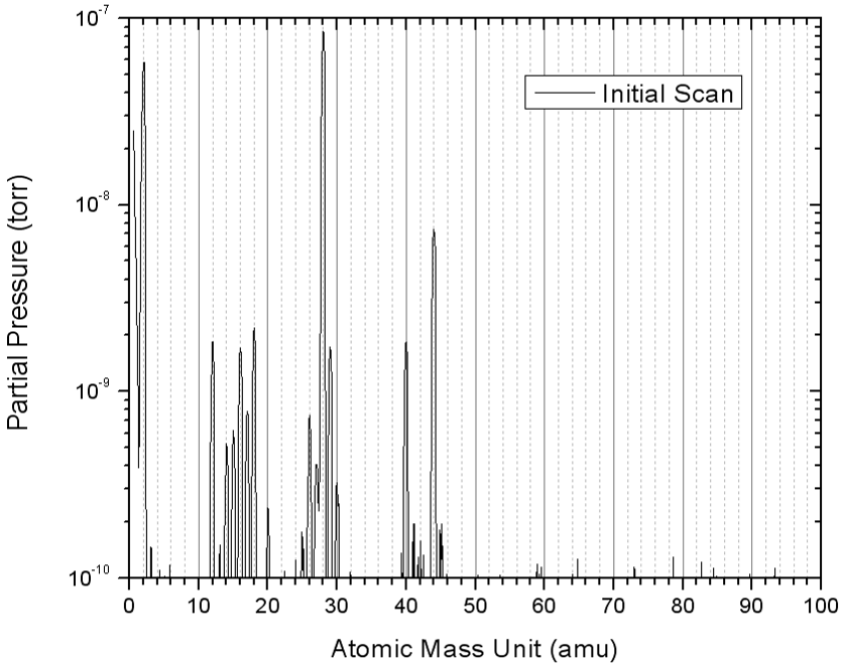

Figure A.1: Mass sweep with residual gases present

Knowing that typical gases in a vacuum chamber include hydrogen, nitrogen, carbon monoxide, methane, and carbon dioxide will help substantially to characterize the residual gases inside. There are many references to typical mass spectra available online and Table A. shows one such resource from Extorr.

Table A.1: Percentage Intensities of Common Mass Peaks

Source → / Mass ↓	Air	Nitrogen	Oxygen	Argon	Water vapor	Hydrocarbon fragment	Carbon dioxide	Carbon monoxide	Hydrogen
1						x			2
2									100
12						x	2	5	
13						x			
14	5	5							
15									
16	1		5		7		5	2	
17					25				
18					100				
20				13					
24						x			
26						x			
28	100	100				x	5	100	
29		1				x			
30						x			
32	25		100						
36						x			
37						x			
38						x			
39						x			
40	1			100		x			
41						x			
42						x			
43						x			
44						x	100		

The mass peak at 28 amu seen in Figure A.1 can be linked to air, nitrogen, and carbon monoxide. The absence of oxygen (O_2) at 32 amu eliminates the air as the source of the mass peak 28. Nitrogen ($N_{2)}$ has a 5% relative peak at 14 amu, which can be seen in the mass sweep of Figure A.1, so N_2 is present. Carbon monoxide (CO) has a 5% relative peak at 12 amu, which is also seen in the mass sweep. This means that the mass peak at 28 amu corresponds to a combination of N_2 and CO. Looking at Table A. again, carbon dioxide also has a mass peak at 12 amu and 44 amu verifying that CO_2 is present in the system. The National Institute of Standards and Technology (NIST) also keep a large database reference guide that lists mass spectra by name or chemical formula.